Special Report to the Tennessee Valley Authority

Evaluation and Testing of Cables Removed from Watts Bar and Browns Ferry Nuclear Plants

TVA Contract TV-82820V

prepared by:
The Electrical Insulation Research Center
University of Connecticut
Institute of Materials Science
Storrs, CT 06269-3136

June, 1991

TABLE OF CONTENTS

LIST OF TABLES

LIST OF FIGURES

1.0 INTRODUCTION

As part of an effort to resolve installation concerns over its safety related cables, the Tennessee Valley Authority (TVA) conducted a series of in-situ high potential (hipot) electrical tests on low voltage control and instrumentation cables installed at its Watts Bar Nuclear Plant (WBN). During the course of that testing several electrical failures of these cables occurred.

It was observed by TVA that a number of the cables that failed during in-situ testing exhibited signs of mechanical damage at the sites where the failures occurred.

A second group of cables that failed during electrical testing did not contain any visible mechanical damage. When these fault sites were located in the laboratory of the Electrical Insulation Research Center (EIRC), no readily apparent cause for the failures could be determined. These cables were identical to another cable recently evaluated by EIRC following a failure during in-situ electrical testing at TVA's Browns Ferry Nuclear Plant(BFN). As a result of subsequent analysis of the WBN cables in this category (which were all obtained from one manufacturer and contract), TVA provided samples of different vintages for comparative analysis. Finally, TVA provided segments from this manufacturer and contract which had failed dielectric testing following the successful completion of loss-of-coolant accident (LOCA) testing. EIRC performed analyses to determine if the apparent cause of these breakdowns was the same as for those which failed the in-situ tests.

Finally, during the course of other activities unrelated to the test program several damaged cables were discovered. No dielectric testing of these cables had been performed in-situ.

At TVA's request, EIRC performed a series of physical, electrical, and chemical tests on the cables listed in Table 1 to determine the probable cause of the damage or, in the case of the non-damaged cables, the probable cause of those breakdowns. Table 2 identifies the breakdown conditions corresponding to the installed cables that failed during in-situ electrical testing.

TABLE 1
INVENTORY OF CABLES ANALYZED

Installed Cables, Watts Bar: 2PV142B, 2PM3926B, 2V1011B, 1PM2485B, 1PM2445B, 1PM2080B, 2PM3806B, 1PM2440B, 2PS207B, 2PM3765B, 1PM1835K, 1PM1381G, 1PM8J, 1PM1232G, 1PM1026G, 1PM1661J, and 1PM1800G

Installed Cable, Browns Ferry: 2RP1945-IB

LOCA-Tested Cables: 01-A-2, 03-A-2, 35-A-2, and 36-A-2

Non-Aged Cables: contracts 79K5-824279-1 and 82K5-830040-2

TABLE 2
INVENTORY AND TEST FAILURE CONDITIONS FOR INSTALLED CABLES

cable	failure conduit	failed conductor	test conditions
2PM3926B	MC914B/MC906B	white	failed 2.5kV dc megger
2V1011B	MC938/MC904	red	failed at 4.1kV dc
1PM2485B	MC880	white	failed at 3.7kV dc
1PM2445B	MC880	black	failed at 3.4kV dc
1PM2080B	MC880	black	failed at 4.9kV dc
2PM3806B	2PM7410B	black, white	failed at 3.6kV dc
1PM2440B	JB5993	black	failed at 3.8kV dc
2PS207B	JB830B	black	failed 2.5kV dc megger
2PV142B	1VC3599B	black	failed at 6.1 kV dc
2PM3765B	JB5989B	white	failed at 4.6kV dc
1PM1835K	JB4042K	black	failed at 3.4 kV dc
1PM1381G	N/A*	N/A	N/A
1PM8J	1PM7254J	black	failed at 3.5kV dc
1PM1800G	N/A*	N/A	N/A
1PM1026G	N/A*	N/A	N/A
1PM1661J	1PM6256J**	white	failed at 1.5 kV dc
1PM1232G	N/A*	N/A	N/A

*note: These cables did not fail, but were found to contain installation damage in conduit 1PM6219G
**note: This identifies the target conduit; refer to text for further discussion of the failure location.

2.0 CABLE IDENTIFICATION

According to a printed label on their jackets, cables 2PM3926B, 2V1011B, 1PM2485B, 1PM2445B, and 1PM2080B were manufactured by Brand-Rex to TVA specifications under contract 80K6-825419, TVA type MS-WVA and MS-WVC, and are of 2 or 4

conductor, #16 AWG, 600 Volt construction. According to data supplied by TVA, cables 1PM2485B, 1PM2445B, and 1PM2080B were originally part of the same cable on reel #1-99352. Cable 2PM3926B was originally obtained from reel #1-000795 and cable 2V1011B was obtained from reel #3-91095. These cables were constructed with a crosslinked polyethylene (XLPE) primary insulation, a tinned copper drain wire, an aluminized Mylar shield, a glass-reinforced silicone rubber composite assembly wrap tape, a Mylar tape layer, followed by a Hypalon® jacket. Several sections of cable were provided for reference purposes. These included sections of the cable, from the same contract, that did not fail during high voltage testing in-situ. In addition, cables from other manufacturers, removed from the same conduits, were provided to EIRC.

Cable 2PM3806B was manufactured by Samuel Moore Corporation, to TVA contract specification 79K5-825874. Upon removal from its conduit, following a high voltage test failure, this cable was noted to contain a significant kink in the area where the fault occurred. This cable was to be examined to determine if the fault could have resulted from physical damage. A 6 in. segment, of the black conductor only, of cable 1PM2440B was submitted for evaluation. No identification marks from the manufacturer were present on the surface of the insulation. At one end of this conductor, a crimp connector was present. This cable was submitted to determine if arcing had occurred at a site that had been cut during installation of a Raychem® insulating sleeve.

A 2.5 in. long section of cable 2PS207B was submitted for evaluation of surface damage. There were no manufacturer's identification marks present on the jacket of this cable section.

According to data provided by TVA, this was manufactured by Anaconda under TVA contract 76K5-87232 and was shipped on reel 1-84. This section of cable was noted to contain a punctured jacket at the approximate mid-point of the length provided. This cable had failed during in-situ high voltage testing at 2.5 kV with a dc megger.

Two sections of cable 2PV142B, approximately 32 in. long combined, were submitted for evaluation of their surface damage. As identified by its jacket labels, this cable was manufactured by Anaconda under TVA contract 81K7-828633. The construction features two #10 AWG conductors, an assembly tape, and no drain wire or shield. An overall jacket was present. The footage marker "34332" was found on the 12 in. section and "34324" was present on the 20 in. long section. The jacket was noted to contain mechanical damage at one site on each of the sections.

An 8 in. long section of cable 2PM3765B was submitted for evaluation of the site where an electrical test failure had occurred. The cable contained no manufacturer's markings since its jacket had been stripped to accommodate a splice sleeve. According to data supplied by TVA, this cable was manufactured by Brand-Rex, under TVA contract 80K6-825419.

A short section of cable 1PM1835K, approximately 8 in. long, was submitted for examination of a puncture in its jacket near one end. This cable was manufactured by Samuel Moore Corp. under TVA contract 77K5-821722. No footage markers were present along the section of cable provided.

Cables 1PM1381G and 1PM8J were manufactured by Samuel Moore Corp. under TVA contract 77K5-821722. The footage markers on cable 1PM1381G ranged from 0001414 to 0001422. This cable contained surface damage, limited to its jacket, near the 0001414 footage marker. The footage markers on cable 1PM8J ranged from 0001958 to 0002004. This cable contained a kink with an associated jacket puncture at footage marker 0001996. In both cases, a characterization of the surface damage was required so that the most likely cause could be determined.

Cables 1PM1232G, 1PM1800G, and 1PM1026G were manufactured by Anaconda Corp. under TVA contract 76K5-87232. Cables 1PM1232G and 1PM1026G were two-conductor cables of type WVA construction. Cable 1PM1800G was of four-conductor, type WVC construction. Cable 1PM1232G contained footage markers ranging from 26656 to 26662. Cable 1PM1800G had footage markers from 09946 to 09954 and cable 1PM1026G contained footage markers from 6054 to 6062. All three of these cables contained jacket damage for which a characterization and probable cause assessment was required.

Cable 1PM1661J was manufactured by Anaconda, under TVA contract 76K5-87232. This cable was received in five sections with one of those sections still installed in a short section of conduit. According to TVA, the cable failed its initial in-situ hipot test but did not re-fail during subsequent testing following segmentation of the cable. The sections were identified by the following footage markers: a) from 17310 to 17324, b) from 17326 to 17342, c) from 17346 to 17350, d) from 17352 to 17354, and e) from 17356 to 17382. The shortest section of this cable was located within conduit 1PM6256 which contained an RTV foam fire

stop at one end. This section of cable was removed from the conduit for testing and inspection.

3.0 VISUAL INSPECTION - ALL CABLES

The failed sections of the cables were first subjected to visual and tactile inspection. Tactile inspection was conducted by running a hand over the surface of the cable to detect any gross irregularities in the texture or overall dimensions. The jacket surfaces were visually inspected for deformation, pinholes, cuts, or other physical damage. Damage was noted on the surfaces of some of the cables shown in Table 2. Cables 2PM3926B, 1PM2485B, 1PM2445B, and 1PM2080B were noted to be free of any discernible surface damage. The jacket surface of cable 2V1011B was noted to contain shallow, broad surface impressions on opposite faces. This area was very flat in appearance and contained no sharp impressions into the jacket at any point. The flattened areas were found between footage markers 02906 and 02910. These could not be photographically recorded using available facilities. The fault site was not visible on the surface of this cable.

Cable 2PM3806B was noted to contain a significant kink approximately 3" away from footage marker 0009392. The jacket at this location was observed to have been torn resulting in the exposure of the insulations of both conductors. Significant charring of the insulations was noted in the area of the kink. The damaged site is shown in Figure 1. Visual examination revealed evidence of surface tracking, conductor melting, and a large eroded area in the overlying aluminum shield tape. Abrasion

damage on the surface of the white insulation and the black insulation was noted.

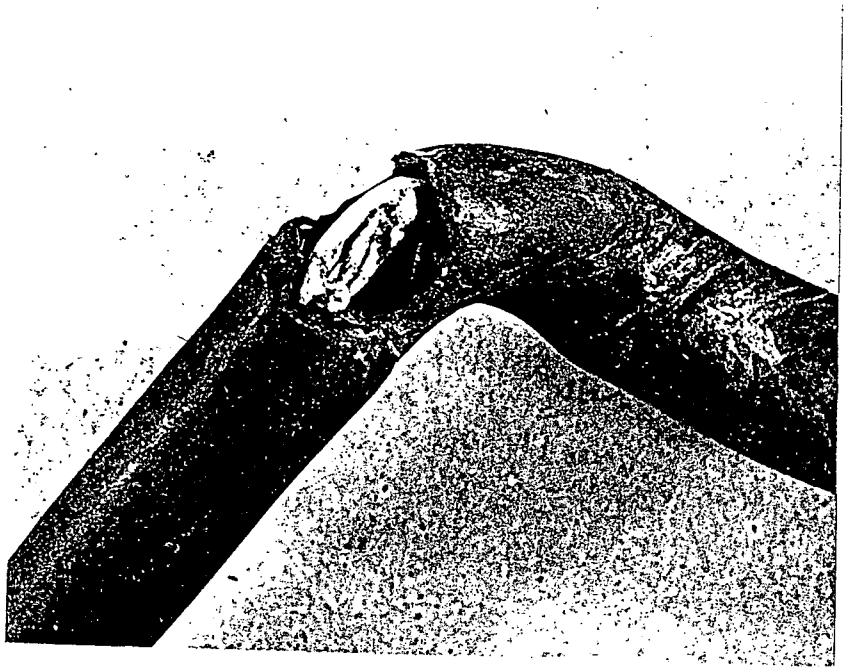

Figure 1. Exposed Mechanical Damage and Fault Site At Location of Kink in Cable 2PM3806B

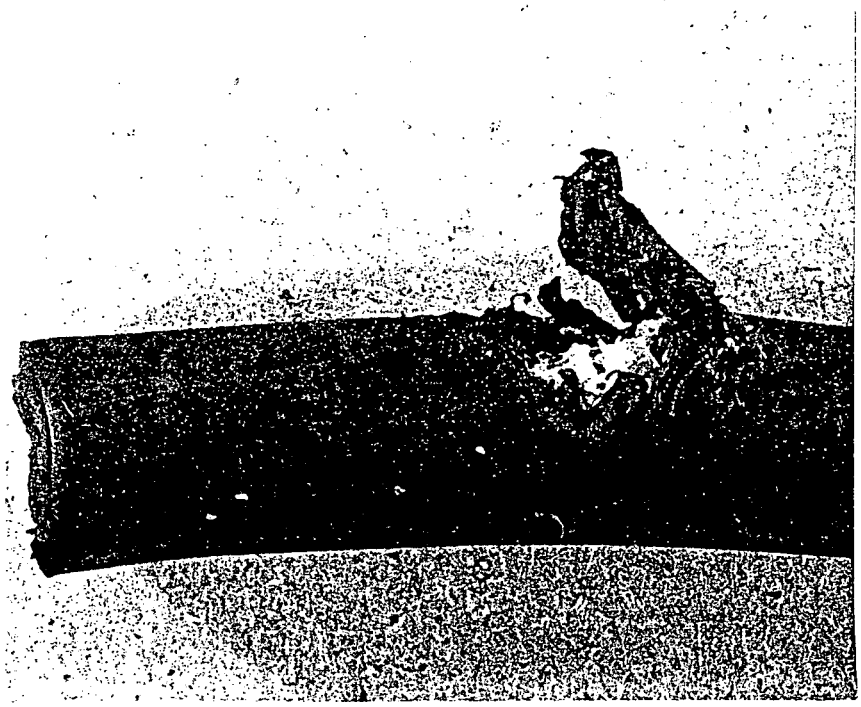

Figure 2. Damaged Site on Cable 2PS207B

Cable 2PS207B was found to contain a series of small cuts in its jacket over a length of approximately 0.45 in. The jacket was observed to be punctured with damage to the underlying shield, assembly wraps, and black insulation, as shown in Figure 2.

Cable 1PM2440B was found to contain a shallow surface cut approximately 2 in. back from the crimp connector and another sharp cut approximately 4 in. behind the crimp connector. The shallow cut was inspected under a stereomicroscope and found to be limited to the outermost surface of the insulation. It was noted by Kent Brown, of TVA, that this shallow cut was previously

located under a Raychem® insulating sleeve. The second cut was inspected with a stereomicroscope and found to penetrate through the insulation to the conductor. This cut appeared to have been made with a sharp instrument. The insulation was pulled back to expose the conductor strands under the cut. At this location, sharp circumferential score marks were noted in the outer surface of two of the conductor strands. The insulation and conductor strands contained evidence of electrical discharge damage at this location. The deep cut, with underlying conductor damage, can be seen on the right side of Figure 3.

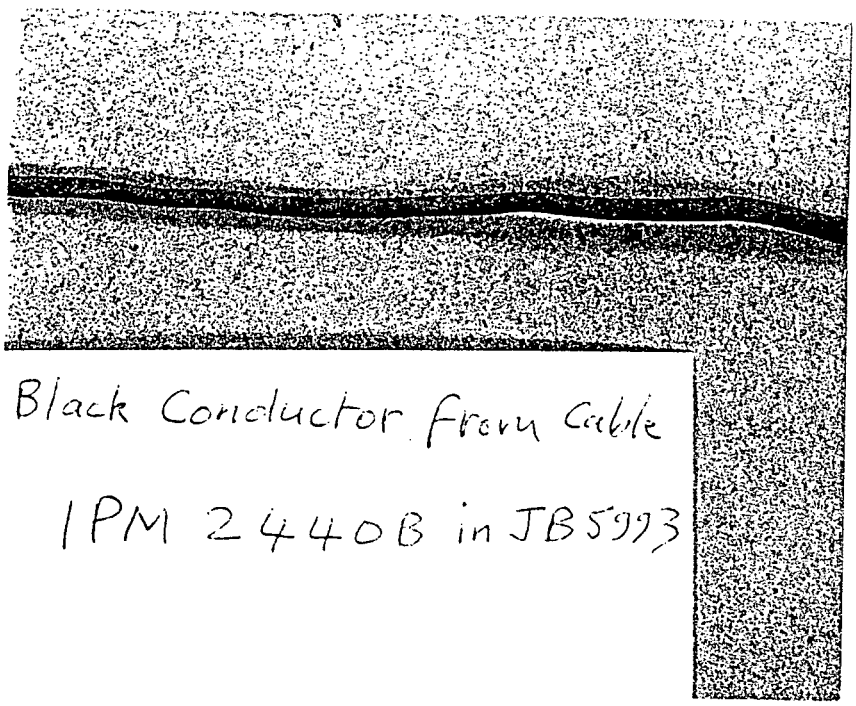

Figure 3. Cuts in Black Insulation of Cable 1PM2440B, Near Crimp Connector

The jacket of cable 2PV142B was found to contain two damaged sites. At the first site, approximately 4 in. away from footage marker 34332, the damage consisted of a series of four parallel, equally-spaced gouges on the outer edge of the cable, adjacent to the white conductor. Their orientation was transverse to the cable length. This damage site is shown in Figure 4. The second damage site, approximately 8 in. away from footage marker 34324, consisted of a longitudinal gouge approximately 1 in. long. At one end, the gouge was very shallow and deepened steadily in one direction, ending with a puncture through the jacket, as shown in Figure 5.

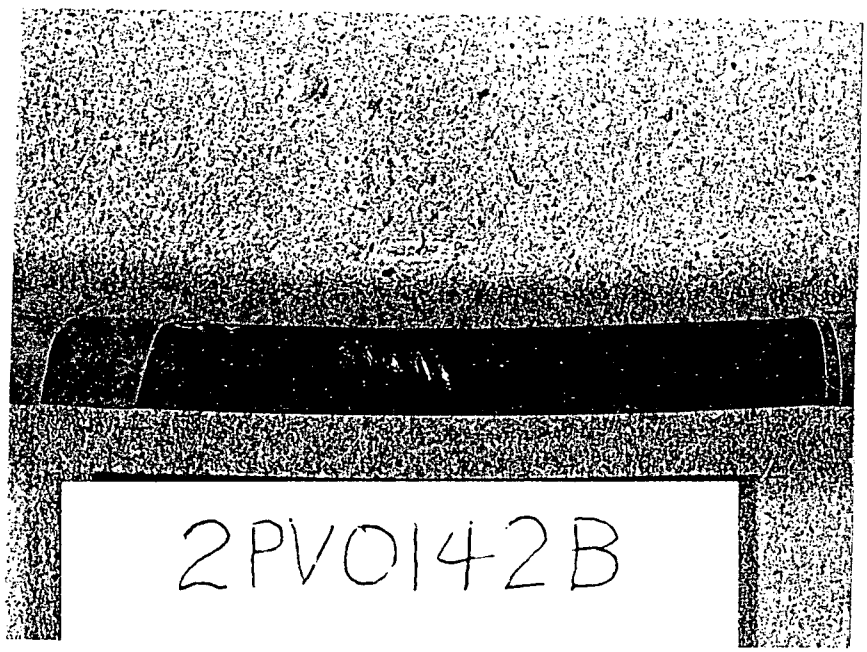

Figure 4. Surface Damage on the Jacket of Cable 2PV142B

Figure 5. Puncture Site in the Jacket of Cable 2PV142B

Cable 2PM3765B consisted of a section that had been stripped to accommodate a splice in its drain wire. A considerable amount of red-colored, elastomeric adhesive was present on the surface in the area of the splice. According to TVA, this was a sealant used under the Raychem® splice sleeve. The latter had been stripped for inspection by TVA prior to being shipped to EIRC for evaluation. The black and white insulations were noted to contain sharp cuts, extending approximately halfway around, near the end of the cut-back in the cable jacket. Electrical discharge damage was evident on the surface of the white insulation only. Below these cuts, shallow corresponding nicks were found in the underlying wire strands. The insulation cuts can be seen on the right side of Figure 6.

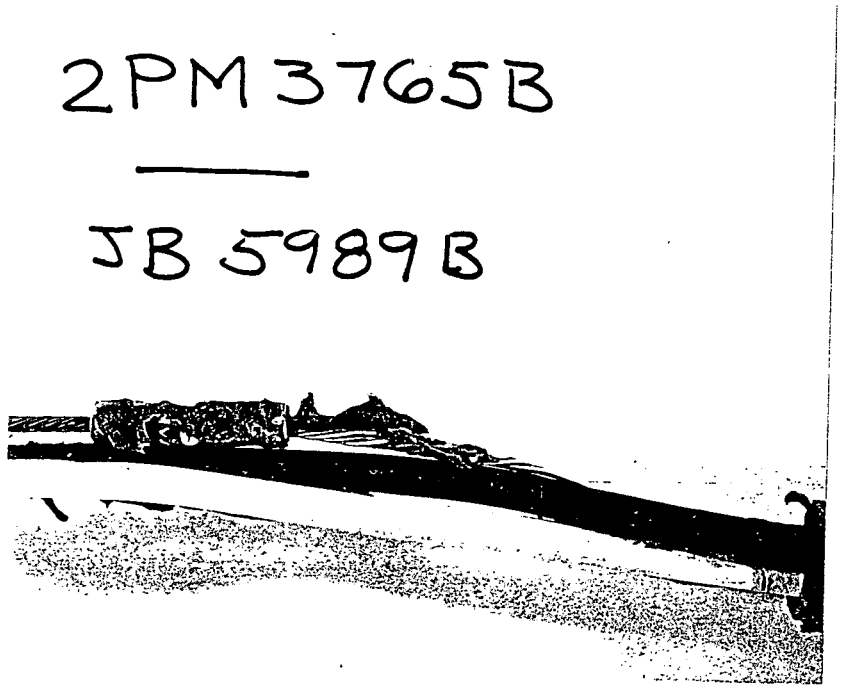

Figure 6. Exposed Insulation Cuts Located Under Repair Sleeve in Cable 2PM3765B

Cable 1PM1835K was found to contain two punctures in its jacket, as shown in Figure 7. The larger of the two consisted of a V-shaped flap, approximately 0.35 in. long. With the stereomicroscope, it could be seen that this penetrated the jacket and that a cut was present through the insulation of the underlying black insulation. Electrical discharge damage was also noted at this site on the black insulation. A smaller puncture was found in the jacket at a location nearly opposite to that of the first puncture. This was limited to the jacket, with no damage to the underlying cable components.

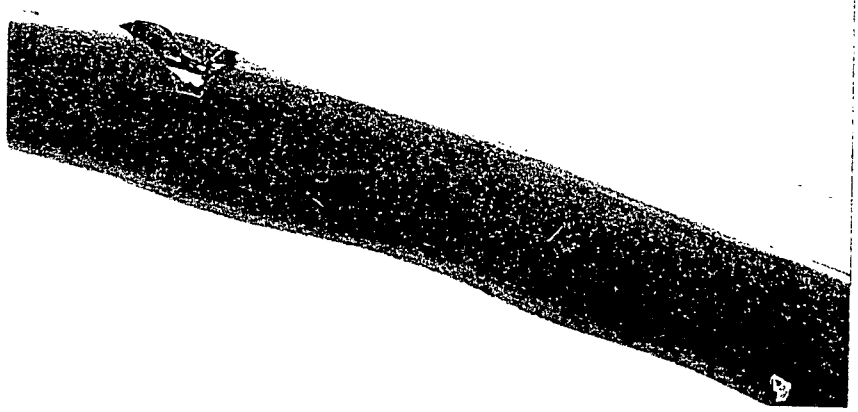

Figure 7. Jacket Damage on the Surface of Cable 1PM1835K

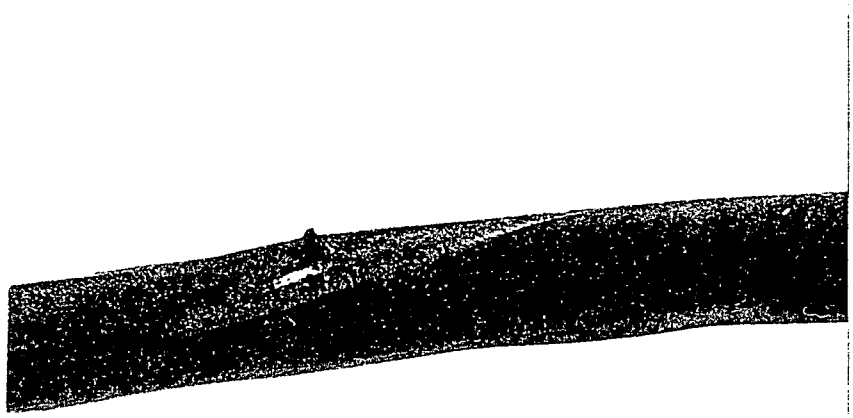

Figure 8. Abrasion Damage on the Jacket Surface of Cable 1PM1381G

Cable 1PM1381G was found to contain a shallow groove in the outer surface of its jacket, as shown in Figure 8. The jacket material was noted to be worn away at this location, with a resulting roughened surface in the bottom of this groove. The groove extended approximately 2 in. along the length of the cable, at approximately the 0001413 footage position. No punctures were found in the jacket at this location.

Cable 1PM8J was noted to be kinked at two spots, located near footage marker 0001996. At the inner radius of one of the kinks, a small puncture was noted in the cable jacket. At the edges of this puncture, transverse wrinkles were noted in the jacket material. This is shown in Figure 9.

Figure 9. Kink and Puncture in the Jacket of Cable 1PM8J

Cables 1PM1232G and 1PM1800G were found to contain shallow grooves in the surfaces of their jackets. The groove in cable 1PM1232G had a nearly flat bottom, with a smooth surface, as shown in Figure 10. There was no evidence of penetration through the jacket. The groove in the jacket surface of cable 1PM1800G was observed to lie at an oblique angle to the length of the cable, as shown in Figure 11. The groove was measured and determined to have a radius of approximately 0.12 in. At no point was any penetration of the jacket surface observed in cables 1PM1232G and 1PM1800G.

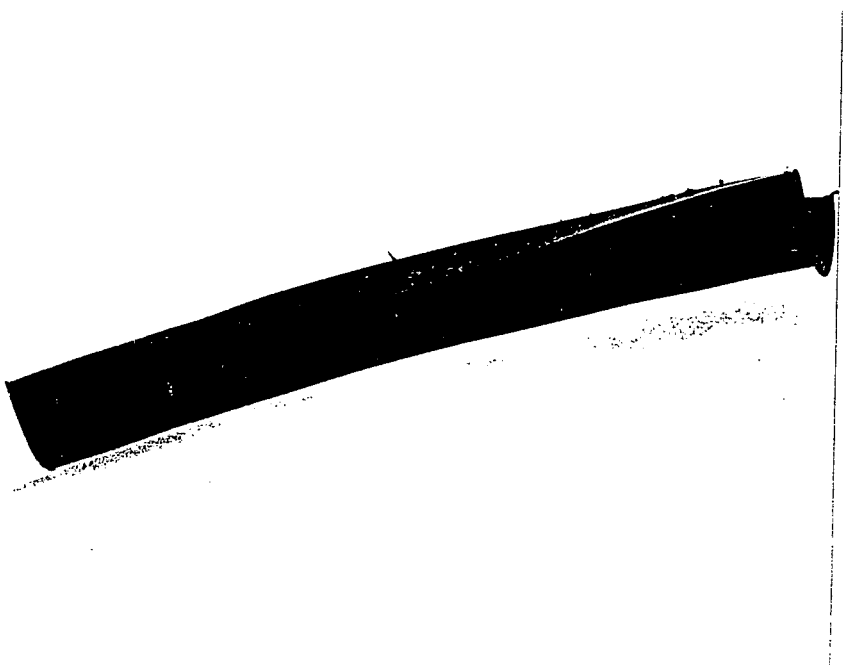

Figure 10. Jacket Damage on Cable 1PM1232G

Figure 11. Surface Damage to the Jacket of Cable 1PM1800G

As shown in Figure 12, cable 1PM1026G contained a groove in its jacket, oriented at an oblique angle to the cable axis. The groove was approximately 0.36 in. wide at its greatest width. At the mid-point of this groove, the jacket was penetrated, with limited damage to the underlying assembly wrap tapes. No conductors were exposed.

Figure 12. Groove in the Jacket Surface of Cable 1PM1026G

The four longest sections of cable 1PM1661J contained only minor surface nicks and scrapes at all locations except one. Approximately halfway between footage markers 17366 and 17368, a 1 in. long diagonal gouge through the jacket was noted. This is shown in Figure 13. This gouge could be seen to have penetrated through the underlying metal shield and assembly wrap tapes. The section of this cable previously contained within the conduit was found to contain a series of small sharp nicks and scrapes on the end that was nearest the RTV foam fire seal. For examination, the cable had been carefully removed from this conduit to avoid inflicting <u>any</u> surface damage. Figure 14 shows this cable and the conduit from which it was removed.

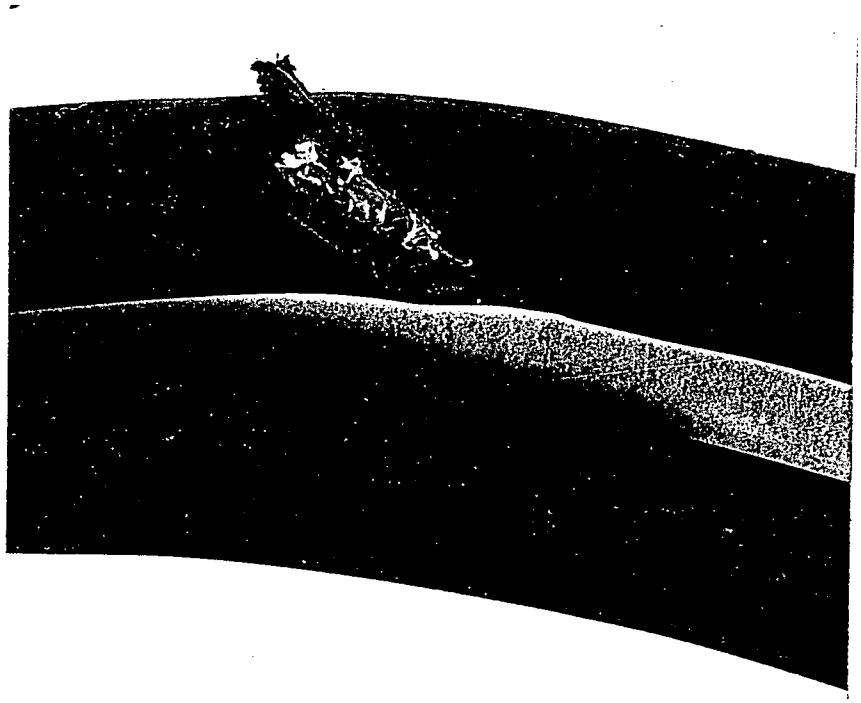

Figure 13. Gouge through the Jacket and Underlying Assembly Wrap Tapes of Cable 1PM1661J

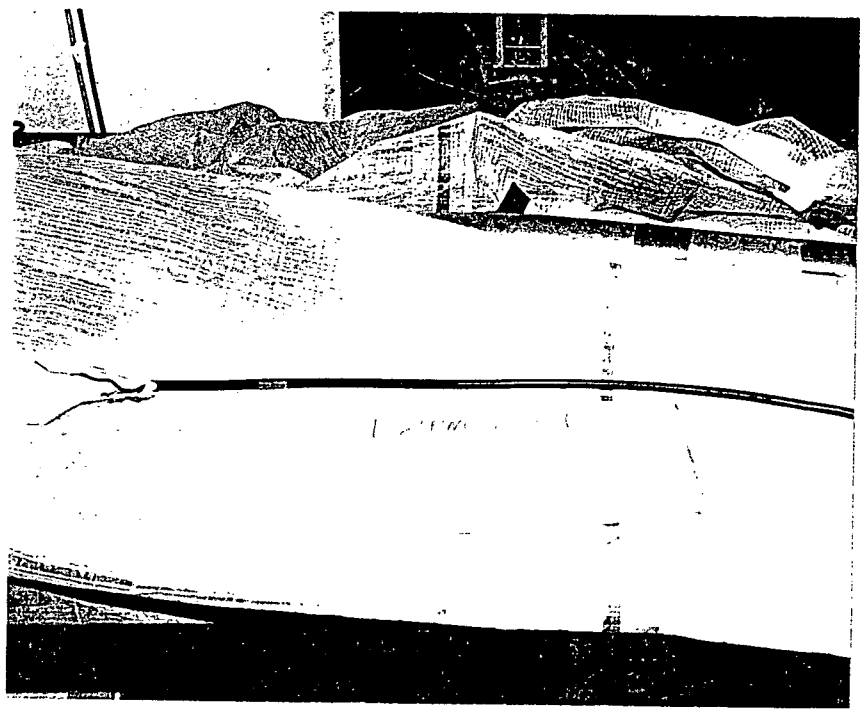

Figure 14. Short Section of Cable 1PM1661J and the Conduit from which it was Removed

4.0 CABLES SUPPLIED TO TVA UNDER CONTRACTS OTHER THAN 80K6-825419

4.1 Dissection and Microscopic Examination

Cable 2PV142B was noted to have failed during in-situ dielectric testing. During visual examination, two sites containing surface damage were noted but there was no corresponding evidence of an electrical failure occurring at either site. At the site of the surface mechanical damage shown in Figure 4, the jacket was sectioned to expose the conductors. No damage was found on the insulation of either conductor or to the overlying assembly wrap tape. The puncture site in this cable, shown in Figure 5, was examined visually and with the aid of a stereomicroscope. The jacket was then dissected to expose the cable components underlying this damaged site. The insulation of the black conductor was observed to contain surface damage, but the conductor was not exposed. This is shown in Figure 15. The gouge and the area immediately surrounding the gouge were found to contain a cluster of glass fibers in a paste-like matrix. The white conductor exhibited no evidence of surface damage. No electrical damage was found at either mechanically damaged site.

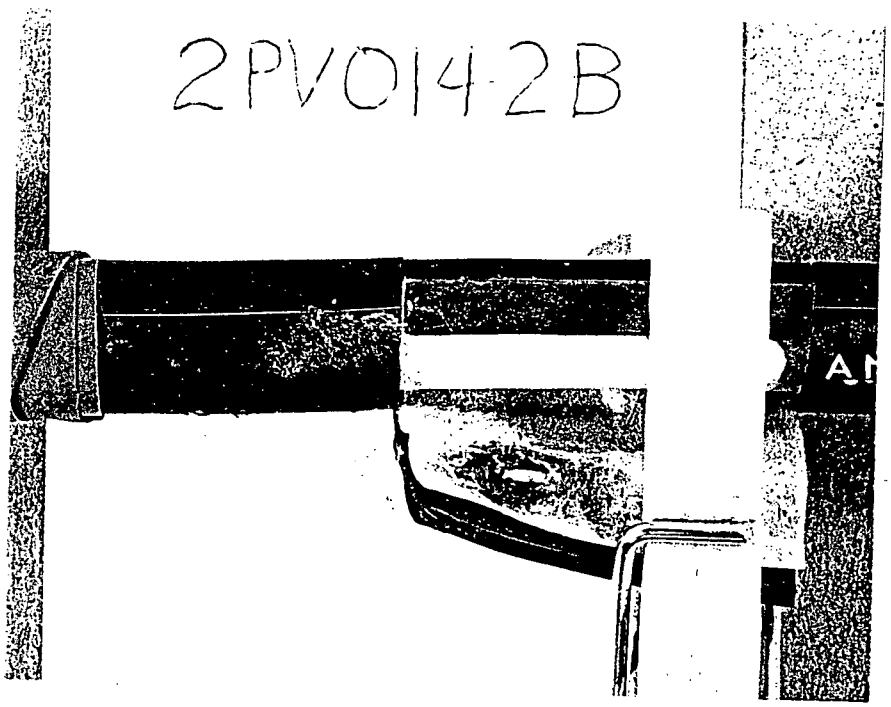

Figure 15. Damage on the Surface of the Black Conductor of Cable 2PV142B

4.2 Results

The fault site in cable 2PM3806B was found to correspond to the location of a severe kink. Mechanical damage of the insulation was located at this site and assumed to have compromised its electrical integrity, thus leading to the fault under in-situ testing conditions.

Since the fault site of cable 2PS207B corresponded to the site of significant mechanical damage, no further analysis was conducted. The cuts were characterized as having been inflicted by a sharp object/instrument. Surface details at the damaged site

suggest that a screwdriver, or similarly shaped tool, may have punctured the cable at this location.

Electrical discharge damage was noted within a small, sharp cut through the insulation of cable 1PM2440B at a location that was not originally contained within the Raychem® insulating sleeve. This cut was determined to have been introduced by a sharp instrument.

At the damage site of cable 2PV142B, nearest footage marker 34324, the damage appears to have been inflicted by the penetration of a tool or other sharp object. From the fiberglass residue found within the gouge, it appears that the object that inflicted the damage was either made with fiberglass or contained fiberglass residues. The damage nearest footage marker 34332 appears to have resulted from high pressure contact with a coarse-threaded surface such as a conduit coupling. The reported failure in this cable was not consistent with the absence of observed electrical damage.

The jacket of cable 1PM1835K appears to have suffered a puncture from a sharp, square-edged tool, such as a screwdriver. The electrical failure in the black conductor of this cable occurred where this instrument caused damage to the insulation.

The jacket of cable 1PM1381G was found to have been abraded. This damage may have resulted from localized high sliding contact force with another cable or pulling rope. The jacket surface of cable 1PM1232G was damaged in a similar fashion.

The kink in the jacket of cable 1PM8J resulted from a mechanical puncture at this location. The cause of the puncture could not be determined.

The jackets of cables 1PM1026G and 1PM1800G contained a groove with characteristics similar to those observed when pull-by damage between similar cables and a "parachute cord" were simulated in the EIRC laboratory. As noted by TVA, parachute cord was found in some of the conduit sections previously occupied by some of the cables identified in this report.

The entire length of cable 1PM1661J was manually stripped of its jacket for the purpose of determining, by visual inspection, where the reported test failure had occurred. In the four longest sections of this cable, no fault sites nor significant mechanically-damaged sites could be found. A Tesla coil was subsequently used to test this section for any small electrical or physical punctures that may have eluded visual inspection. No such sites were located with this method. Test records subsequently availed to EIRC indicated that the test failure on this cable had occurred in the section contained within conduit 1PM6256J. Following its removal from the conduit, this section of cable was subjected to insulation resistance measurements. These were first conducted with an applied potential of 500V dc and the resistance was measured individually for each conductor with respect to the drain wire. The insulation resistance values were approximately 2×10^{12} ohms and the measurements remained stable in excess of five minutes. These measurements were repeated with an applied potential of 1000V dc and the measurements were virtually identical. This section of cable was then stripped of its jacket and subjected to visual examination to determine where the test

failure had occurred. No fault site could be located. Electrical testing of the exposed insulations using a Tesla coil was unable to detect a fault site. The jacket damage found between footage markers 17366 and 17368 was inspected under the stereomicroscope. At this location, the jacket was stripped to expose the underlying cable insulations. No damage was found to any components other than the jacket, metal shield, and assembly wrap tapes. The reported test failure of cable 1PM1661J is inconsistent with the observed absence of a fault site. Based on previous jacket damage simulation experiments conducted at EIRC, the jacket damage present between footage markers 17366 and 17368 was most likely caused by sliding contact with a parachute cord.

Dissection of the mechanically damaged site on cable 2PM3806B revealed some electrical damage to the white and black conductors. This damage indicated surface arcing between the shield tape and both conductors. The electrical damage occurred at sites where the insulations had been peeled due to the mechanical damage that occurred where the cable had been kinked. This is shown in Figure 16.

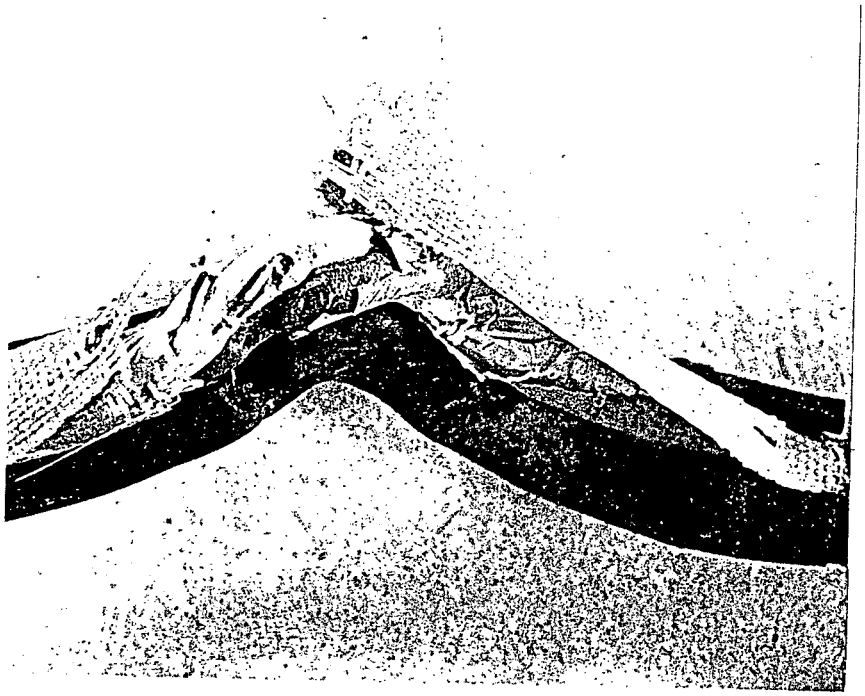

Figure 16. Exposed Fault Site in Cable 2PM3806B

5.0 CABLES PURCHASED ON TVA CONTRACT 80K6-825419

5.1 Electrical Tests

A Tesla coil was used to determine if any radial faults or pinholes through their jackets might have been present in cables 2PM3926B, 2V1011B, 1PM2485B, 1PM2445B, or 1PM2080B. For each cable, the individual conductors were separately grounded while the Tesla coil was passed over their surfaces to detect discharge sites. None were found using this method. It should be recognized that the capacitance of the lengths of cables used for this test would significantly limit the current available for creating an arc.

Cables 2V1011B, 1PM2485B, 1PM2445B, and 1PM2080B were then subjected to high voltage testing using a Hipotronics model 730/15-40 PR parallel resonance test set. Each cable was first placed into wooden isolation brackets then each conductor was separately energized with the remaining conductor(s) and drain wires grounded to a common point. The applied potential was monitored using a Fluke model 37 digital voltmeter equipped with a Fluke 50kV high voltage test probe. Voltage was applied to the conductors at a rate of 1kV/minute. The occurrence of a breakdown was noted by a sharp increase in the transformer secondary load. The breakdown voltage varied from sample-to-sample and the results are summarized in Table 3. Immediately following breakdown, the corresponding sites were located by manually locating the hot spot on each of the cables. These sites were then marked for subsequent dissection and analysis.

TABLE 3
SUMMARY OF BREAKDOWN VOLTAGES AND FAULT SITE LOCATIONS

cable	breakdown voltage, kVac	breakdown site, (footage)
2V1011B	1.7	02908
1PM2485B	2.5	00242
1PM2445B	1.7	00438
1PM2080B	1.9	00904

Cable 2PM3926B was shipped in three sections and it was not known in which of these sections the test failure had occurred. It is EIRC's understanding that this cable was cut at three locations to minimize its physical damage during removal. Without

knowing which section might contain the fault, insulation resistance measurements were first conducted with a Hewlett-Packard model 4329A high voltage resistance meter to attempt to determine which section contained the fault site. Measurements were made between each conductor and the drain wire, then from conductor-to-conductor. Measurements were conducted at applied potentials of 100V and 1000V DC. The latter voltage represents the output limit of the instrument. The results of these tests are shown in Table 4. Throughout the tests, the insulation resistance values remained high and stable. There were no indications in which section a fault site might have existed.

Cable 2PM3926B was then subjected to high voltage testing using the protocol previously described. Both conductors (white and black) in each of the three sections were able to withstand 10kVac for one minute. Based on this protocol, no fault site was found in any section of this cable using these methods. No further examination or analysis of this cable was conducted to date.

The sections of cable 2PM3926B noted in Table 4 can be identified with their respective TVA labels, as follows. Section 1 was noted as "from condulet, conduit MC906". Section 2 was labelled "LB condulet C10/P/741, 1st cut". Section 3 was labelled "from end PNL-2-R-140, EL 708".

TABLE 4
INSULATION RESISTANCE MEASUREMENTS, CABLE 2PM3926B

conditions	applied potential	resistance, ohms
section 1, white to drain	100V	2.5×10^{10}
section 1, white to drain	1000V	1.8×10^{10}
section 1, black to drain	100V	2.5×10^{10}
section 1, black to drain	1000V	1.2×10^{10}
section 1, white to black	100V	2.3×10^{10}
section 1, white to black	1000V	2.0×10^{11}
section 2, white to drain	100V	2.0×10^{10}
section 2, white to drain	1000V	2.2×10^{10}
section 2, black to drain	100V	2.0×10^{10}
section 2, black to drain	1000V	1.6×10^{11}
section 2, white to black	100V	5.0×10^{10}
section 2, white to black	1000V	1.6×10^{11}
section 3, white to drain	100V	2.3×10^{10}
section 3, white to drain	1000V	1.8×10^{11}
section 3, black to drain	100V	2.5×10^{10}
section 3, black to drain	1000V	1.0×10^{11}
section 3, white to black	100V	2.4×10^{10}
section 3, white to black	1000V	1.8×10^{10}

5.2 Visual and Microscopic Examination

The locations corresponding to the hot spots in cables 2V1011B, 1PM2485B, 1PM2445B, and 1PM2080B were visually examined for signs of exterior damage. None was found at any of these locations. Though a complete visual examination had been conducted at EIRC prior to high voltage testing, subsequent examination, now confined to the identified fault locations, was conducted to verify whether any surface damage was evident. No

bulges or irregularities in the cable dimensions could be felt by hand. The fault locations on each cable were then dissected, layer-by-layer, and inspected. Photographic records were prepared during this procedure, showing each layer of cable components as they were exposed. Since no anomalies were noted at locations other than those noted in this report, photographs of those areas were not included in this report but will be transferred to TVA. The fault sites were then inspected with a stereomicroscope to determine if any localized defects could be found that might explain the isolated nature of the failures. Within the burned areas, the cable components were examined for dimensional irregularities. The conductors were inspected to determine if any broken strands were present or if any irregularities in the strand bundles resulted in sharp protrusions. These, if present, could have served to increase the local electrical stresses thus explaining the fault occurrence. A description of the fault sites in each of the cables follows.

As previously noted, cable 2PM3926B contained no fault site that could be located with the methods available.

Cable 2V1011B was noted earlier in this report to contain shallow surface impressions on opposing faces of the cable jacket. These impressions were determined to have a depth of approximately 1 mil. Dissection and inspection of the fault site underlying these impressions revealed that arcing had occurred between the red conductor and the drain wire, as shown in Figure 17. Two small flattened areas were noted on the red conductor immediately adjacent to the fault site. These were found on opposite faces of this wire. An additional, single small flat spot was noted on the surface of the black wire, in the area immediately adjacent to the

fault site. All three flattened areas were located at the same position along the cable. No other physical or construction anomalies were noted at this fault site.

Figure 17. Exposed Fault Site in Cable 2V1011B

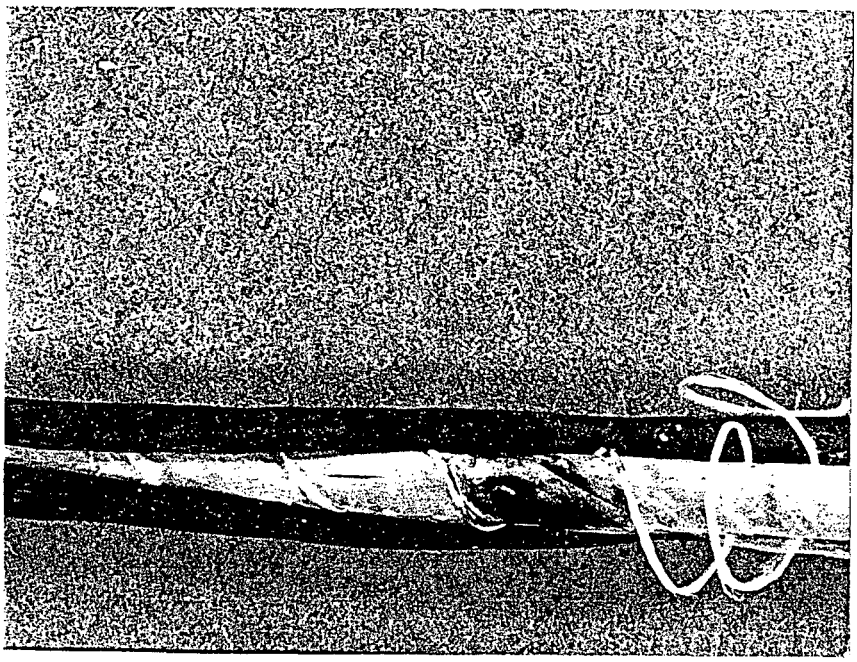

Figure 18. Fault Site in Cable 1PM2485B

Cable 1PM2485B contained a radial fault between the white conductor and the drain wire and shield, as shown in Figure 18. There were no physical or construction anomalies at this site visible with the stereomicroscope. Cable 1PM2445B contained a similar radial fault between the black conductor and the drain wire, as shown in Figure 19. There were no physical or construction anomalies noted at this fault site.

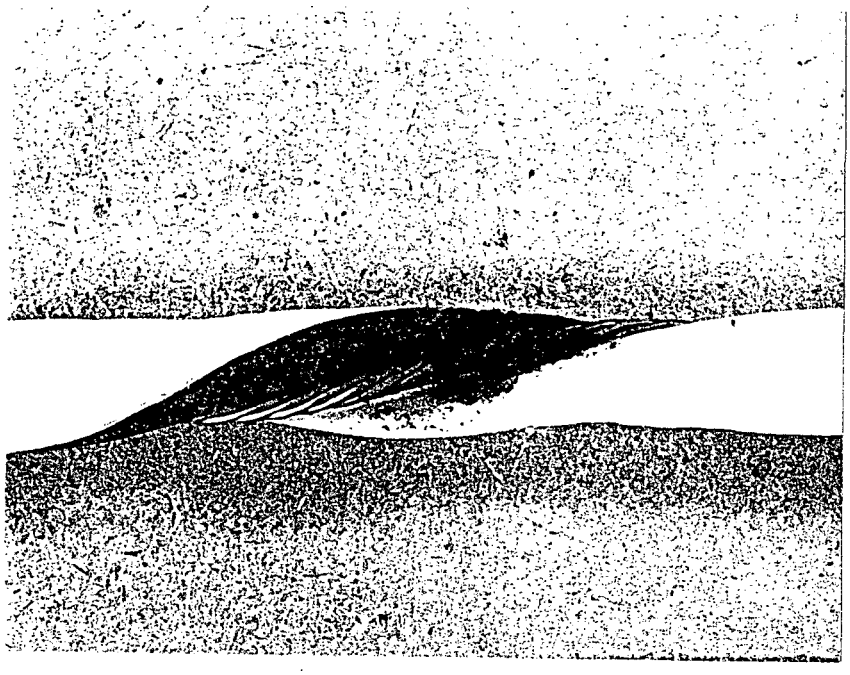

Figure 19. Fault Site in Cable 1PM2445B

Cable 1PM2080B was found to contain a narrow, radial electrical puncture directly between the black conductor and the shield. This is shown in Figure 20. The puncture had a diameter of approximately 15 mils. No evidence of mechanical damage or

construction anomalies in the cable components could be found at this location.

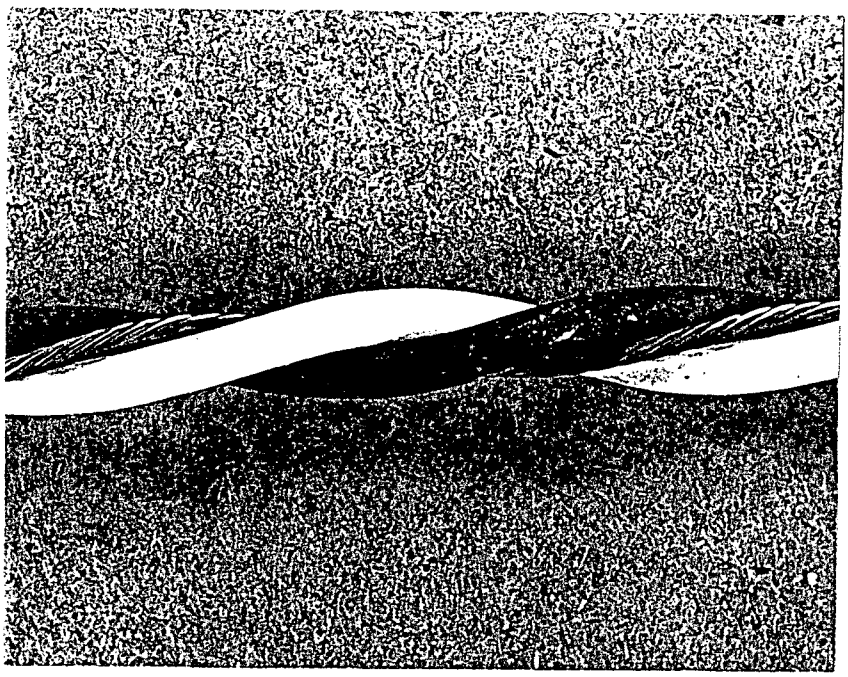

Figure 20. Fault Site in Cable 1PM2080B

Electrical tests were not conducted on cable 2PM3765B since the fault site was readily located. Microscopic inspection of this cable indicated that it had sustained arcing damage at the site of a cut in the insulation that was most likely inflicted when the jacket was stripped back for a splicing operation.

5.3 Physical Measurements

The wall thickness and hardness of the insulations within each cable were measured and comparisons between these properties at the faulted and non-faulted sites were made. Samples from the fault site were tested at a location as near these sites as could be obtained without encountering charred material. The areas away from the fault corresponded to a location 1 in. away from the center of each fault. Table 5 summarizes the hardness measurements. ASTM method D2240 was followed for all insulation hardness tests. Shore hardness D and A scales were used, as required.

TABLE 5
HARDNESS MEASUREMENTS OF CABLE INSULATIONS
SHORE A OR D VALUES, AVERAGED FOR THREE LOCATIONS

		hardness	
cable	cond. color	near fault	away from fault
2V1011B	white	----	A97.5
2V1011B	black	----	A97.7
2V1011B	red	A97.7	A98.5
2V1011B	green	----	A98.2
1PM2485B	white	A97.8	A97.8
1PM2485B	black	----	A97.7
1PM2445B	white	----	A97.2
1PM2445B	black	A96.7	D64.5
1PM2080B	white	----	A96.5
1PM2080B	black	A98.3	A94.3

The insulation wall thickness was measured for each conductor at a location 1 in. away from the fault area for each of the cables. The average values for maximum and minimum insulation

wall thickness are presented in Table 6. From these measurements, it is clear that there are no anomalies in the insulation wall thickness. In addition, the cables passed the TVA specification for minimum insulation wall thickness.

TABLE 6
INSULATION WALL THICKNESS MEASUREMENTS COMPARING FAULTED AND NON-FAULTED AREAS OF SAME CABLE

		thickness, mils	
cable	cond. color	minimum	maximum
2V1011B	white	27.6	29.1
2V1011B	black	27.6	29.9
2V1011B	red	27.6	29.9
2V1011B	green	28.3	29.9
1PM2485B	white	28.3	29.9
1PM2485B	black	27.6	31.5
1PM2445B	white	27.6	30.7
1PM2445B	black	27.6	30.7
1PM2080B	white	27.6	29.9
1PM2080B	black	28.3	29.9

5.4 Chemical Analysis

As noted during the analysis of cable 2RP1945-IB from the Browns Ferry nuclear plant, reported by EIRC on August 23, 1990, anomalies were found within the inorganic components of the insulation at the fault site. Since five of the cables in the present evaluation were manufactured under the same contract, an evaluation of the inorganic constituents was again conducted. In this case, chemical analysis of the materials found at the fault site was performed, along with similar analysis of the material extracted from the Browns Ferry nuclear plant cable.

Small sections of the charred insulation from one half of the fault site were removed from cables 2V1011B, 1PM2485B, 1PM2445B, and 1PM2080B and subjected to high temperature exposure in a vacuum oven to separate the insulation polymer from the inorganic constituents present in the insulation compound. The remaining half of the fault site was preserved. For comparison purposes, sections of insulation from the same conductors, approximately 4 in. away from the fault site, were prepared in identical fashion. This preparation method, referred to as pyrolysis, was accomplished by placing each insulation section into an alumina crucible, followed by exposure to 605°C temperature under vacuum in a Ney-Barkmeyer model II vacuum furnace. The material remaining in the crucibles after this treatment was then examined under a stereomicroscope. Measurements were made to determine the particle sizes and photographs were prepared to document selected particles.

The pyrolysis residues from the insulations at the fault sites were found to contain a number of large particles. The largest particles were of two distinct types, based on their appearance. The first consisted of irregularly-shaped brilliant white particles, such as the one shown in Figure 21. The other type consisted of large particles with a mottled gray-black appearance. Figure 22 shows one particle of this type. The residue from the fault site of cable 1PM2485B was found to contain gray-black particles with a high aspect ratio (ratio of major to minor dimension). The largest of these particles had an overall length of 59 mils, a width of 14 mils, and a thickness of approximately 6 mils. Five similar particles from this cable ranged in dimensions from 3 x 9 x 16 mils to 2 x 3 x 4 mils. In

the residue, a number of white particles were also found. The largest of these was 3 x 14 x 15 mils.

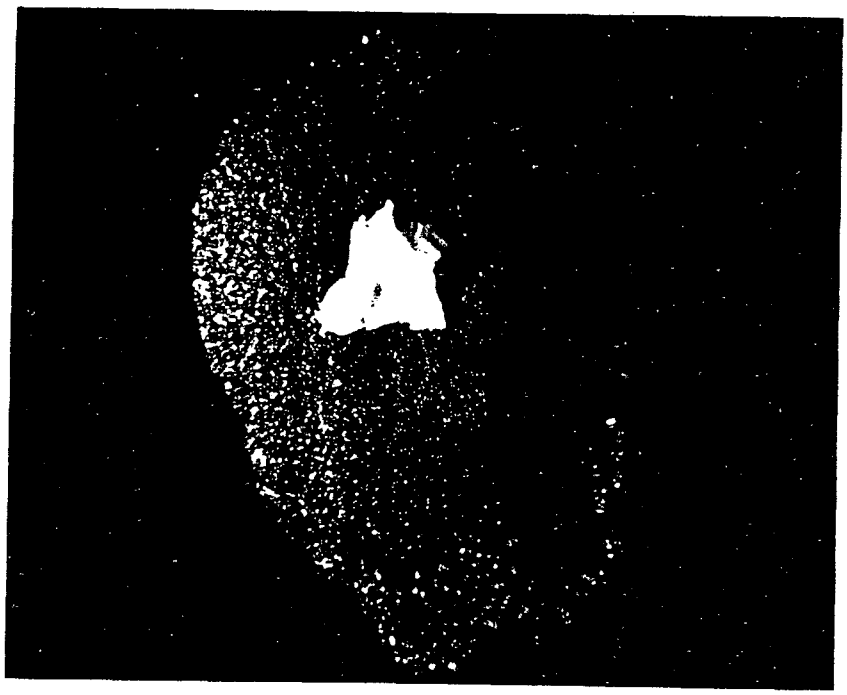

Figure 21. White Particle Removed from the Insulation at the Fault Site of Cable 2V1011B

Figure 22. Gray-Black Particle Removed from the Insulation at the Fault Site of Cable 1PM2485B

The pyrolized residue from the fault site of cable 2V1011B contained a mixture of gray-black particles and some bright white particles. The largest of the gray-black particles had dimensions of 6 x 22 x 33 mils. Others ranged in size from 3 x 17 x 19 mils to 2 x 3 x 10 mils. The largest of the white particles had dimensions of 6 x 11 x 11 mils.

The pyrolysis residue from Browns Ferry cable 2RP1945-IB was examined with a stereomicroscope and found to contain large gray-black particles and a number of smaller white particles. The largest gray-black particle had dimensions of approximately 5 x 10

x 12 mils. The largest white particle had dimensions of approximately 4 x 8 x 11 mils.

Similar examination of the pyrolysis residue from the insulation approximately 4 in. away from the fault site showed similar materials present, but the maximum particle size was determined to range from approximately 4-10 mils in major dimension. In the case of cable 2V1011B, the residue from the non-fault site contained only white particles with a maximum dimension of 4 mils. The non-fault site of cable 1PM2485B contained mostly gray-black particles with a maximum dimension of 6 mils.

Representative large particles removed from the fault sites of cables 2V1011B and 1PM2445B were chemically analyzed using X-ray emission spectroscopy. This method combines a scanning electron microscope (SEM) with an X-ray spectrometer to enable chemical analysis of particles approximately 0.2 mils diameter, or larger. The SEM is an instrument used to examine fine structures and is capable of image magnification in excess of 100k. This uses a finely focused electron beam that is scanned over the surface of a specimen. Electrons scattered back from the surface and others emitted by the specimen through secondary processes are used to produce an image. Since the electrons are sufficiently energetic to strip electrons from the sample, X-rays are emitted from the area undergoing electron bombardment. By determining the energy of the X-rays emitted by the specimen, they can be identified with the elements from which they arose. Particles for this analysis were prepared by mounting them into a high purity carbon paint as seen surrounding the particle in Figure 21. Due to the small size of these particles, this operation was conducted

under a stereomicroscope. The specimens were then coated with a thin layer of gold using a vacuum sputtering technique. The latter process was required to render the surfaces of the particles conductive. Non-conductive specimens would accumulate a high voltage charge in the SEM which would serve to electrostatically deflect the electron beam. The gold layer was approximately 50 Ångstroms thick and, at this thickness, is transparent to the electron beam and not detectable by the X-ray spectrometer. For the bulk of these examinations, an AMRay model 1810 SEM and EDAX model PV9800 X-ray spectrometer were used.

In addition to the particles from cables 2V1011B, 1PM2445B, 1PM2485B, and 1PM2080B, the particles previously removed from Browns Ferry cable 2RP1945-IB, conduit 2RP1917-IB, were analyzed using X-ray microanalysis procedures. Table 7 summarizes the results of the elemental analyses. For comparison purposes, non-pyrolized areas of the insulation from the corresponding cables were analyzed at two locations to provide an overall assessment of the insulation composition. This information is also presented in Table 7.

TABLE 7
ELEMENTAL ANALYSIS OF PYROLYSIS EXTRACTS FROM INSULATIONS CABLES 2RP1945-IB (BROWNS FERRY), 2V1011B, 1PM2445B, 1PM2485B, AND 1PM2080B

cable	particle type	elements present
2V1011B	gray-black A, loc. 1	Al, Si, Sb, Ti, Cu
2V1011B	gray-black A, loc. 2	Al, Si, Sb, Ti, Cu
2V1011B	gray-black A, loc. 2	Al, Si, Sb, Ti, Cu
2V1011B	gray-black B, loc. 1	Al, Si, Sb, Ti, Cu
2V1011B	gray-black B, loc. 2	Al, Si, Sb, Ti, Cu
2V1011B	gray-black B, loc. 3	Al, Si, Sb, Ti, Cu
2V1011B	white, loc. 1	Si
2V1011B	white, loc. 2	Si
2V1011B	white, loc. 3	Si
1PM2445B	gray-black, loc. 1	Al, Si, Sb, Cu
1PM2445B	gray-black, loc. 2	Al, Si, Sb, Cu
1PM2445B	gray-black, loc. 3	Al, Si, Sb, Cu
1PM2445B	white, loc. 1	Si
1PM2445B	white, loc. 2	Si
1PM2445B	white, loc. 3	Si
2V1011B	non-pyrolized, loc.1	Al, Cl, Sb, Br
2V1011B	non-pyrolized, loc. 2	Al, Cl, Sb, Br
1PM2445B	non-pyrolized, loc. 1	Al, Cl, Sb, Br
1PM2445B	non-pyrolized, loc. 2	Al, Cl, Sb, Br
2RP1945-IB	gray-black, loc. 1	Al, Si, Sb, Ti, Cu
2RP1945-IB	gray-black, loc. 1	Al, Si, Sb, Ti, Cu
2RP1945-IB	gray-black, loc. 1	Al, Si, Sb, Ti, Cu
2RP1945-IB	white, loc. 1	Si
2RP1945-IB	white, loc. 2	Si
2RP1945-IB	white, loc. 3	Si
1PM2485B	gray-black A, large area	Al, Si, Sb, Ti, Cu
1PM2485B	gray-black B, large area	Al, Si, Sb, Ti, Cu
1PM2080B	gray-black A, large area	Al, Si, Sb, Ti
1PM2080B	gray-black A, large area	Al, Si, Sb, Ti, Cu

The fault sites of cables 2V1011B, 1PM2440B, 1PM2485B, 1PM2080B, and 2RP1945-IB (Browns Ferry) were found to contain a

number of atypically large particles of inorganic materials. As noted in Table 7, the white particles consisted of silicon and the gray particles contained aluminum, silicon, antimony (Sb), with, in some cases, copper (Cu) and titanium (Ti). Figures 23 and 24 are X-ray analysis spectra corresponding to white particles from the fault site of cable 1PM2445B and a gray-black particle from the insulation at the fault site of the same cable, respectively. It should be noted that silicon, aluminum, titanium, and copper are all most likely present as oxides. This conclusion is based on the optical characteristics of these materials. The X-ray emission spectroscopy method used for the bulk of the particle analyses is not capable of detecting oxygen. Antimony, chlorine, and bromine are components of the flame retardant system in these cables, as described by the manufacturer, whose technical representative was present when these analyses were conducted. Titanium is an ingredient of many colorant systems used to color-code conductors. The source of silicon has not been unequivocally determined. The manufacturer stated that this is not a normal ingredient of the insulation system and this was verified based on analysis of the insulations, as cited in Table 7 and shown in the X-ray analysis spectrum corresponding to a non-pyrolized area of the insulation from cable 2V1011B, as shown in Figure 25. Copper found in the fault sites is presumed to have originated from evaporation of the copper conductor during the electrical discharge event. X-ray spectra not presented in this report will be provided to TVA.

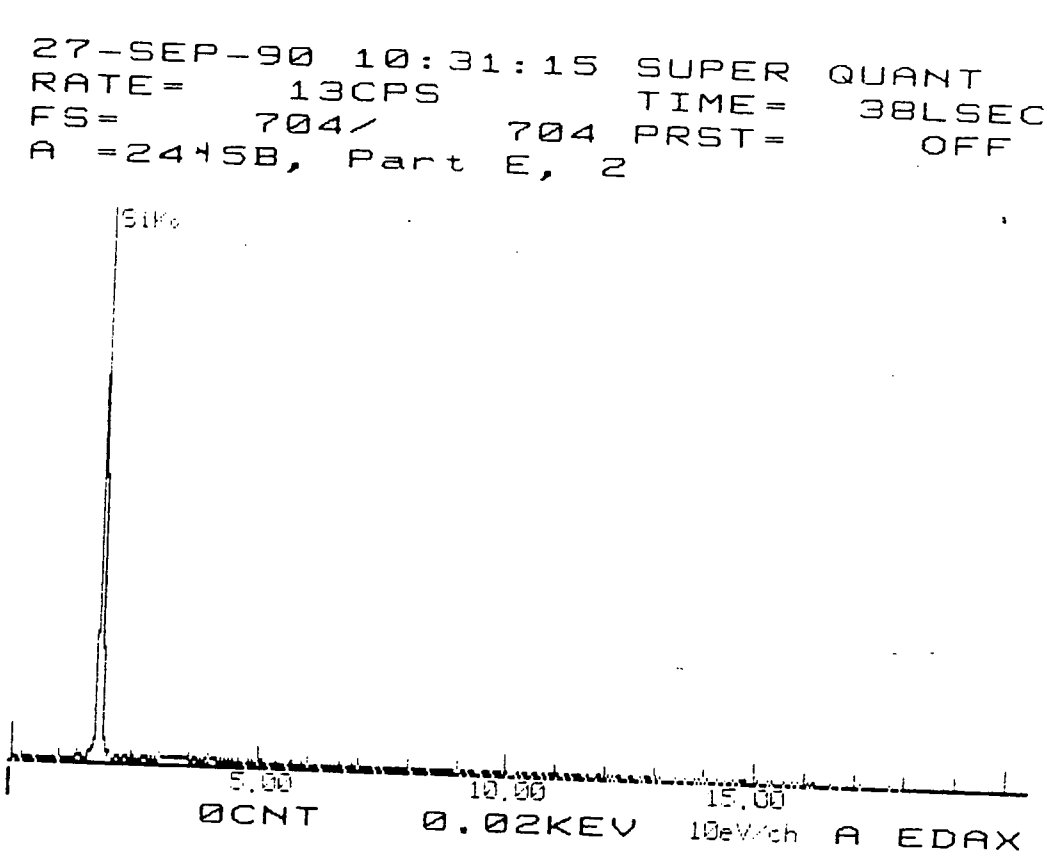

Figure 23. X-ray Analysis Spectrum Showing the Composition of a Large White Particle Removed from the Insulation at the Fault Site of Cable 1PM2445B

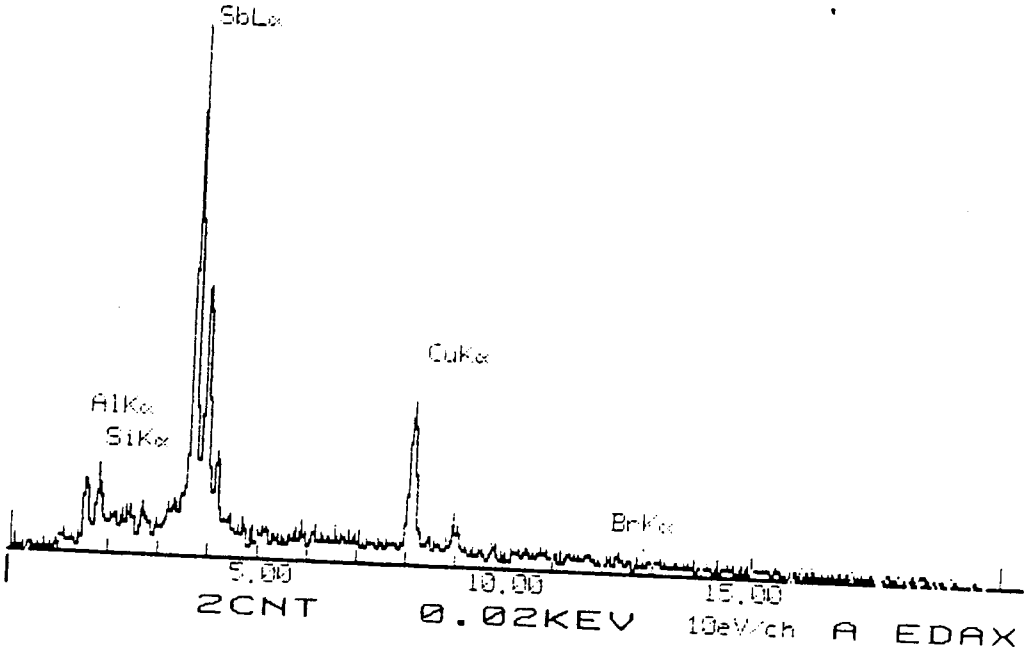

Figure 24. X-ray Analysis Spectrum Showing the Composition of a Large Gray-Black Particle Removed from the Insulation at the Fault Site of Cable 1PM2445B

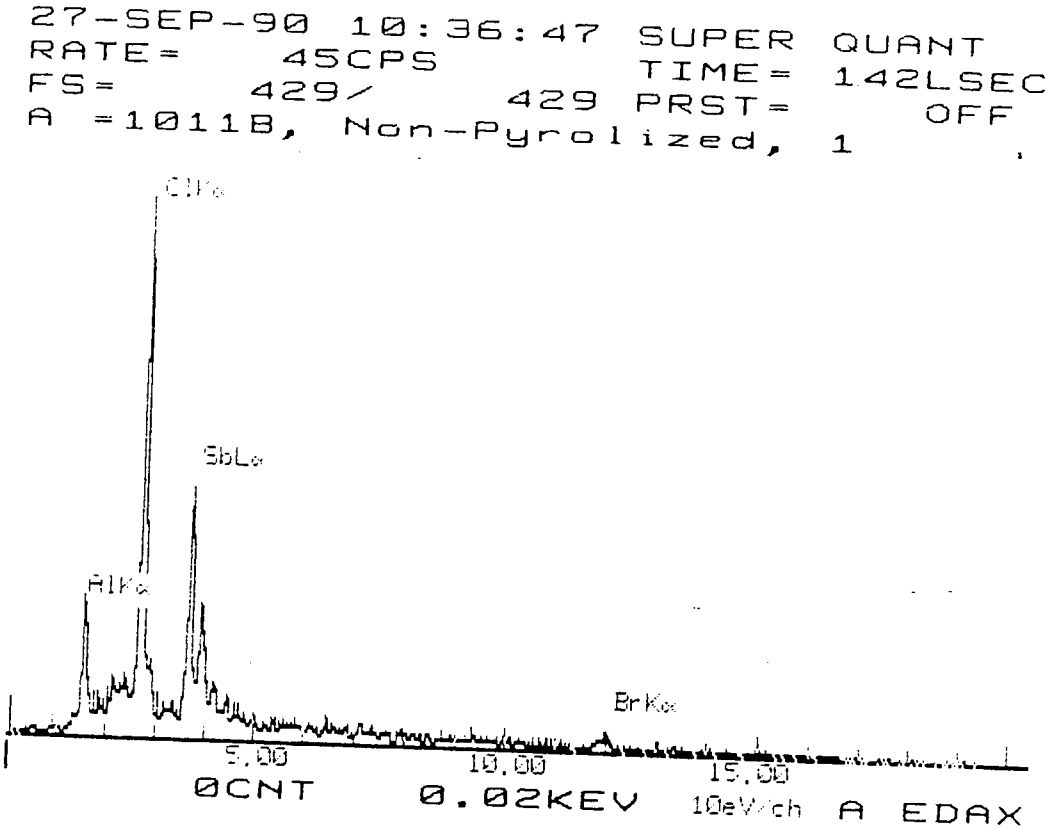

Figure 25. X-Ray Analysis Spectrum Showing the Composition of Non-Pyrolized Insulation from Cable 2V1011B

5.5 Manufacturer's Concerns

The source of silicon in the pyrolysis residues from the cables previously described was initially attributed by the manufacturer to the glass fiber-reinforced silicone rubber assembly tape. It was stated that during the fault event and/or during pyrolysis of the cable insulations, sufficient heat may have been present to convert the components of the tape into silicon dioxide. To test this hypothesis, sections of this assembly tape were removed from cables 1PM2080B, and 2RP1945-IB and subjected to pyrolysis conditions identical to those used for pyrolysis of the insulations near the fault sites of the affected cables. These included vacuum pyrolysis at 605°C. Following pyrolysis it was found that the silicone rubber component of the

tape had evaporated leaving no residue that could be detected using a stereomicroscope. The glass fibers were found to have been unaffected by this treatment. Alternatively, the manufacturer suggested that the silica may have been produced from thermal decomposition of a silicone-based processing aid (lubricant) that is used during extrusion of the insulation compound. A sample of this fluid could not be obtained. Based on EIRC's experience this would most likely be a methyl- or phenyl-siloxane oil which would decompose into volatile products if exposed to 605°C temperature.

To address a concern that the observed large particles of insulation constituents may have been formed during the fault or during subsequent high voltage testing of the cables, the following experiment was conducted. A length of cable 2PM3920B was selected. This had been manufactured under the same contract as the others that had failed during high voltage dc testing for reasons other than mechanical damage. This length of cable had passed dc high voltage testing in-situ. The cable was divided into two sections and first tested to 10 kVac. Both sections passed this test. Next, a pinhole was placed through the jacket and into the insulation of one of the conductors in each cable using an 11 mil diameter stainless steel wire. The cable sections were then subjected to high voltage ac testing at a rate of rise of 1 kV/min. Punctures resulted at the pinhole sites. The insulation at these sites was subsequently pyrolized and the ash was examined under the stereomicroscope. Though some fairly large gray-black and white particles were found in the pyrolysis residue, these were considerably smaller than those found in the faults produced during in-situ testing. The largest particle found in either fault site measured 4 x 6 x 14 mils. It should be

noted that the observed large particles in the insulation at the fault sites from laboratory simulation and in-situ testing were of a very sharp, angular morphology. Had these particles formed by thermal fusion, a spherical morphology would be expected.

The manufacturer expressed an additional concern that the atypically large inorganic particles found near the fault sites of the affected cables may have resulted from fusion of the inorganic particles in the insulation compound during the fault event or during the heating that resulted from the methods used by EIRC to locate the fault sites. To test this hypothesis, a series of tests were conducted to study the effect of a range of elevated temperatures on the morphology and size of antimony trioxide particles from the insulation of these cables. Sections of the insulation from cable 2PM3920B were subjected to pyrolysis at 620°C, 650°C, 660°C, 750°C, 1100°C, and 1300°C. The temperatures were chosen according to the following considerations. Pyrolysis of all fault sites was conducted at 605°C $\pm$ 2°C. Lower temperatures could not be used since a minimum of 600°C is required to remove the polymer. Since 656°C is the melting point of antimony trioxide (CRC Handbook of Chemistry and Physics, 1989), temperatures below and above this point were used to determine what effect this treatment would have on the size and shape of the antimony trioxide particles from the insulation. Since copper was detected by X-ray microanalysis in the fault site residues, it is reasonable to assume that the conductor melting temperature (1083°C) was reached (CRC Handbook of Chemistry and Physics, 1989). For this reason, temperatures slightly above this point (1100°C) and well above this point (1300°C) were used. Pyrolysis at 620°C and 650°C failed to introduce any changes in the size and shape of the antimony trioxide particles compared to

these properties when pyrolysis was conducted at 605°C. When a pyrolysis temperature of 660°C was used, the particles were observed to have fused into a number of round particles, as shown in Figures 26 and 27. No sharp edges were observed on any of the particles formed through this process. At temperatures of 1100°C and 1300°C, the antimony trioxide evaporated.

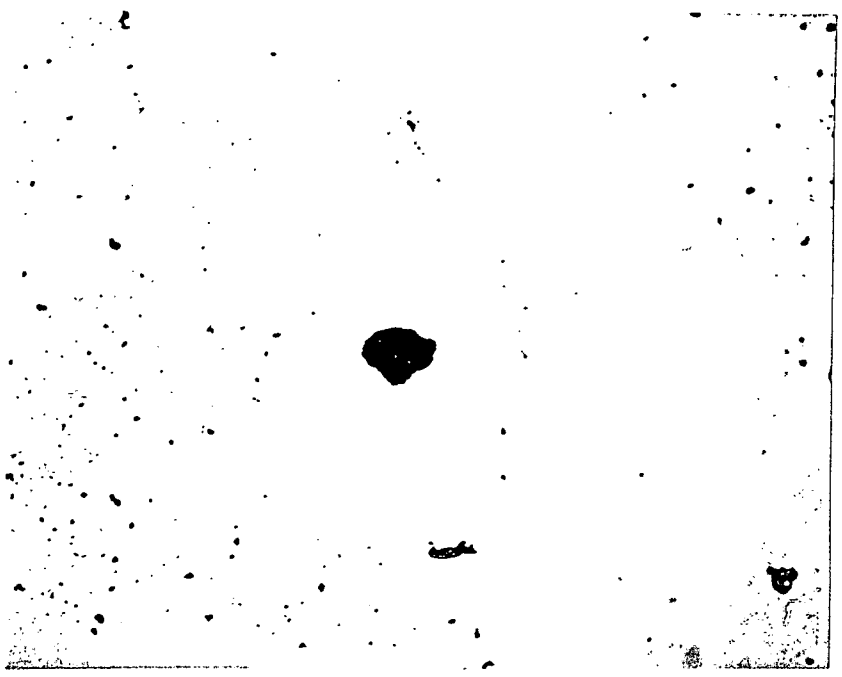

Figure 26. Antimony Trioxide Particles Following Pyrolysis at 660°C

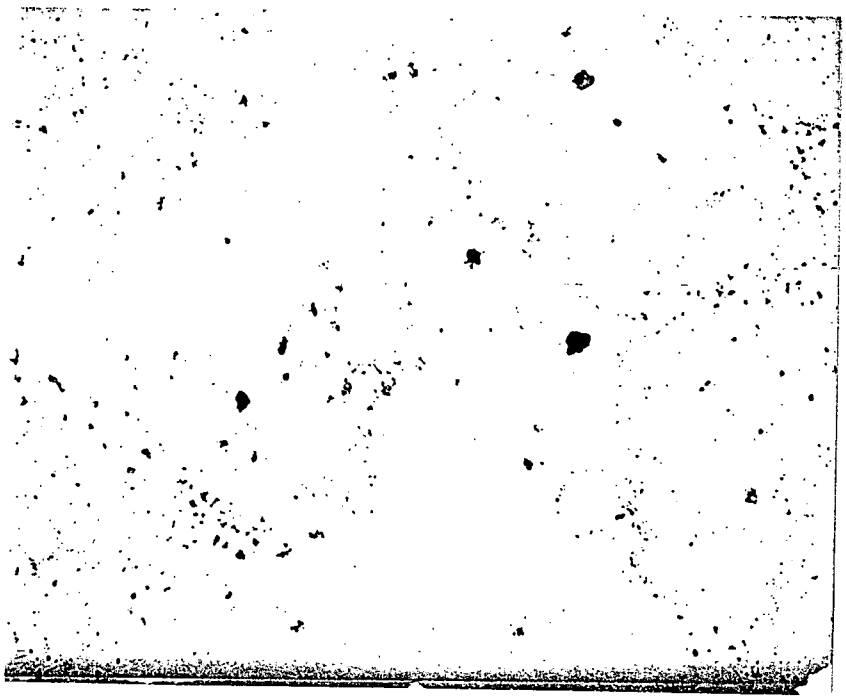

Figure 27. Antimony Trioxide Particles Following Pyrolysis at 660°C

5.6 Morphological Examination

Microtomed sections of insulations from the area near the fault sites of cables 1PM2445B, 2V1011B, and 1PM2080B were prepared and examined using optical microscopy techniques. This method was used to determine if any abnormally large particles of the inorganic constituents could be located within the insulation, using non-pyrolized samples. The largest particle in cable 1PM2445B was found in the black conductor and this had a maximum dimension of 3.9 mils. During examination of one of the microtomed sections of this insulation, a large crater was noted

with a length of 25 mils. Due to the irregular texture of the inner surface of this crater and the presence of gray-black residue on the inner surface, it is possible that a large particle or agglomerate pulled out of this location during the microtoming operation. No particles larger than 4 mils could be found in the insulations of cables 2V1011B and 1PM2080B. It should be noted that the opaque nature of these insulations limited optical microscopic examination to the near surface of a microtomed slice. It was not possible to determine if the particles visible through the microscope were complete or merely small cross-sections of larger particles. For this reason, it is desirable to separate the particles from the polymer matrix. Since the insulations of these cables were manufactured with crosslinked polyethylene, solvents could not be used to isolate the polymer and inorganic constituents. Pyrolysis is one alternative method that can be used. Examination of the microtomed sections was performed on the off-chance that a large particle could be seen, if present. In addition, such examination was useful to determine if voids were present within the insulation. The presence of voids would have offered a possible explanation about why the faults had occurred in these cables.

5.7 Comparisons with Other Brand-Rex Contracts

5.7.1 Introduction

After anomalous large particles of antimony trioxide and silica within the insulation were determined to be associated with in-situ high voltage dc test failures, a series of analyses were undertaken to determine if there were significant differences between the insulation compounds of various vintages provided by the same manufacturer. The manufacturer had stated to TVA that

identical insulation formulations were used for various vintages of this type of cable. Since failures were limited to a specific vintage and contract, it became necessary to determine if the observed large particles of primarily antimony trioxide were unique to the insulation from the cables manufactured under contract 80K6-825419. It is noted that in-situ high voltage dc test failures did not occur in the cables supplied under contracts 79K5-824279-1 and 82K5-830040-2, those selected for comparison purposes. As described in the following sections, a series of analytical tests were undertaken to assess the mechanical, chemical, and morphological (structural) properties of the insulation compounds from cables of these vintages.

5.7.2 Analysis Procedures

Mechanical tests were conducted to determine the tensile strength and elongation limits of the insulation compounds from cables supplied under contracts 79K5-824279-1, 80K6-825419, and 82K5-830040-2. Strips of the insulations with a thickness of 10 mils were prepared with a sledge microtome, manufactured by Spencer Lens Company. These were subsequently trimmed to obtain specimens with nominal dimensions of 10 mils thickness, 20 mils width, and 2.5 in. length. These were then fixed into an Instron model 1000 tensile testing system with Instron fiber grips. The specimens were pulled at an extension rate of 2.0 in./minute. Extension of the specimens was measured by determining the crosshead deflection through use of a built-in linear variable differential transformer, with a resolution of less than 0.1 mil. Load was monitored with a 10 lb load cell with a resolution of 0.02 lb. Ten specimens from the insulation of each cable were analyzed in this fashion. The procedures of ASTM D882 and D1708

were followed for these tests, with the exception of the sample size. There is presently no available ASTM standard for testing thin specimens of the type used in these tests. Due to the constraint imposed by the thin cable insulations, thicker specimens could not be used.

Shrink-back tests were conducted for an overall assessment of the extrusion conditions under which several of the cables that experienced in-situ test failures were manufactured. Shrinkage behavior is also an indication of some basic properties of the insulation compound. For these tests, sections of cables with a length of 12 in. were prepared. The ends were prepared so that all components were of the same length, with resulting parallel end faces. The cables were then placed into an air convection oven at 60°C and periodically examined and measured for evidence of insulation shrink-back. Cables 2V1011B, 1PM2485B, 1PM2445B, and 1PM2080B were subjected to these tests. Sampling intervals of 24, 48, 144, and 312 hours were used.

Density measurements were conducted on four insulation specimens from four cables that had experienced in-situ test failures and from two specimens of other vintages. Density measurements provide information about variations in the overall composition of the insulations. For example, if the concentration of inorganic components were to change from location-to-location in a given cable, density measurements would reflect these changes. In addition, density can also be affected by the extrusion conditions, thus density measurements may also reflect variations in processing conditions. These tests were conducted using a density gradient column, filled with water/calcium bromide mixtures. Insulation sections were approximately cubic in shape,

with a volume of approximately 2×10^{-3} in^3. The procedures of ASTM method D-1505 were followed for these measurements and National Institute of Standards and Technology (NIST) density standards were used for calibration. Areas near and away from the fault sites of cables 2V1011B, 1PM2080B, 1PM2485B, and 1PM2445B were analyzed and compared to insulations provided to TVA under contracts 79K5-824279-1 and 82K5-830040-2. The areas near the fault sites of the cables cited above were obtained within 1 in. of the fault sites in all cases. Those areas away from the fault sites were obtained from distances of several feet or more from the center of the fault sites on the corresponding cables.

The degree of crosslinking of the cable insulations was determined through solvent extraction methods, using ASTM Procedure D-2765-84. A section of each cable insulation approximately 2 in. long was divided into a number of smaller sections, each weighed with an analytical balance, then placed into a Soxhlet extraction apparatus, filled with reagent grade xylene. Extraction was conducted with boiling xylene (145°C) for approximately 24 hours. Following this, the samples were vacuum dried at 60°C for 24 hours to remove the solvent, then weighed again. The change in weight was used to calculate the soluble non-crosslinked portion of the insulation. As will be explained, it was necessary to determine the proportion of inorganic constituents within the insulation so that the total amount of crosslinked polyethylene could be determined. The net weight of the polymer was used as the basis for crosslinking density calculations.

Infrared spectroscopy was used to chemically analyze the insulation components extracted from the insulation for the

crosslinking density measurements previously described. Spectroscopic analyses were conducted to determine if any differences could be found between the cable vintages with respect to their extractable organic components, such as an antioxidant. The solvent extracts from the crosslinking density determinations were used in all cases. This extract was concentrated onto a sodium chloride plate, heated to accelerate drying of the solvent, followed by application of additional extract. Approximately 25 ml of each extract was concentrated in this manner, then subjected to analysis using Fourier transform infrared spectroscopy.

Thermogravimetric analysis was used to quantitatively compare the insulation compositions near and away from the fault sites of selected cables that had failed during in-situ testing. This method was also used to compare the compositions of these insulations with those provided under contracts 79K5-824279-1 and 82K5-830040-2. Thermogravimetric analysis (TGA) was used to determine the change in weight of a small sample of insulation as a function of increasing temperature. With this method, a sample of insulation weighing approximately 5-10 mg was inserted into a precision analytical balance mounted within a temperature-programmable furnace. The furnace is enclosed within a quartz tube to allow the test to be conducted within a user-selected gas environment. Typically, nitrogen is used to determine changes in weight that are not associated with oxidation, while an oxygen atmosphere is used to determine those changes that are associated with oxidation. TGA analysis provides a continuous plot of weight vs. temperature and a decrease in weight occurs when the decomposition and/or evaporation temperature of each component within a sample is reached. For example, water is typically evolved at about 100°C, polyethylene at approximately 280-290°C,

and carbon black at 600°C. Comparisons between TGA plots of similar compounds can be used to determine if differences in formulation are present. A heating rate of 10°C/min was used for TGA analysis of the insulations. Insulation samples within 1 in. of the fault sites were compared to areas approximately 4 in. away from the fault sites from the corresponding cables. TGA was also used to compare the insulation composition along the length of cable 1PM2485B. The latter tests were conducted to determine if there were significant differences in the local composition of the insulations near the fault sites of the affected cables. Analyses were conducted on 10 insulation samples removed at 0.25 in. increments, beginning within 0.5 in. of the fault site.

The morphology of the cable insulations was directly examined with a polarizing microscope. For examination with this instrument, thin sections of the insulation were prepared so that light could be transmitted through the material to enable observation of the distribution, size, and orientation of the inorganic components within the insulations of the cables that failed during in-situ testing. A microtome was used to prepare thin sections of the insulations from sites near the fault and approximately 4 in. away from the fault sites on the failed cables. Comparative observations were made of the insulations from cables manufactured under contracts 79K5-824279-1 and 82K5-830040-2. Magnifications ranging from 40x through 200x were used to examine the insulation morphology. All dimensional measurements were made with a calibrated eyepiece scale which was tested using a NIST-certified standard with a resolution of 0.1 μm. The polarizing microscope used for this work was equipped with a camera so that permanent photographic records could be prepared.

Since pyrolitic separation of the inorganic constituents of the cable insulations had been called into question by the cable manufacturer, it was decided that an alternate method would be used to examine representative and subsequent specimens. For this application, oxygen plasma etching was employed. This process uses a radio frequency-generated plasma of pure oxygen gas to slowly etch organic materials. In this process, the oxygen plasma attacks the polymer by converting it to carbon dioxide gas. The system used for these procedures is a model 5500 plasma etcher manufactured by Polaron Instruments. This system has a maximum output power of 150 Watts and produced a surface temperature of no more than 70°C during the etching process applied to these cables. This system required more than 6 hours to fully remove the polymeric component from an insulation sample. Insulations from cables supplied under contracts 79K5-824279-1 and 82K5-830040-2 were subjected to plasma etching to isolate the inorganic components for subsequent examination and measurement. The insulations from cables 2V1011B and 1PM2445B were similarly treated.

Measurements of particle size were conducted directly, using the procedures previously described, and through use of a computerized image analysis system. The latter uses a computer, coupled to a microscope, to facilitate measurements of a large number of particles. The image analyzer divides an image into digital bits, each of which has a size that is calibrated using a NIST-certified reference scale. Particles in a field of view, for example, are measured by adding the number of calibrated bits that lie within its boundaries. The system can recognize the maximum length of a particle by measuring the image bits along a line that is rotated through uniform azimuthal increments, until a maximum

dimension is found. Systems of this type may be used to measure hundreds of particles per minute. The particle size distributions of the inorganic constituents of the insulations from cables 2V1011B and 1PM2445B were analyzed in this fashion and compared with insulations from cables supplied to TVA under contracts 79K5-824279-1 and 82K5-830040-2. A Dapple/Mac image analysis system was used for these measurements.

5.7.3 Results

Tensile and elongation measurements of the insulations are summarized in Table 8. For those cables that failed during in-situ testing, the insulations away from the fault sites had an average tensile strength of 1492 psi and an average elongation limit of 218%. For the same cables near their fault sites the average insulation tensile strength at break was 1470 psi with an average elongation limit at break of 198%.

TABLE 8
TENSILE AND ELONGATION LIMITS AT BREAK OF INSULATIONS FROM VARIOUS CABLES/LOCATIONS

cable	location	footage marker	elong., %	tensile strength, psi
2V1011B	away from fault	02928	217	1403
2V1011B	near fault	02910	194	1457
1PM2080B	away from fault	00880	241	1426
1PM2080B	near fault	00904	233	1422
1PM2485B	away from fault	00210	225	1546
1PM2485B	near fault	00240	169	1477
1PM2445B	away from fault	00448	189	1594
1PM2445B	near fault	00436	196	1522
79K5-824279-1	random	04582	246	1901
82K5-830040-2	random	00452	284	1734

TABLE 9
SHRINK-BACK CHARACTERISTICS OF CABLE INSULATION VS. EXPOSURE TIME AT 60°C

	change in length, mils			
cable	24 hrs	48 hrs	144 hrs	312 hrs
2V1011B	0.0	0.0	0.0	0.0
1PM2485B	0.0	0.0	0.0	0.0
1PM2445B	0.0	0.0	0.0	0.0
1PM2080B	0.0	0.0	0.0	0.0

Shrink-back tests of the insulations of the cables shown in Table 9 indicated that none showed any measurable tendency toward longitudinal deformation after extended periods at elevated temperature.

TABLE 10
INSULATION DENSITIES FOR SELECTED CABLE SAMPLES AND LOCATIONS

cable	location	footage	density, gm/cm^3
2V1011B	away from fault	02928	1.2269
2V1011B	near fault	02910	1.2104
1PM2080B	away from fault	00880	1.2519
1PM2080B	near fault	00904	1.2636
1PM2485B	away from fault	00210	1.2551
1PM2485B	near fault	00240	1.2618
1PM2445B	away from fault	00448	1.2669
1PM2445B	near fault	00436	1.2593
79K5-824279-1	(non-aged cable)	04582	1.2559
82K5-830040-2	(non-aged cable)	00452	1.2419

Density measurements were conducted on the insulations from the cables shown in Table 10. The results listed in this table are the averages obtained from ten replicates for each cable/location. This table also shows the footage marker on the corresponding cable nearest the locations from which the insulation samples were obtained. Densities of the insulations from the cables that failed during in-situ testing were similar to those from the cables made during 1979 and 1982 by the same manufacturer. Comparison of the densities of the insulations near and away from the fault sites of cables 1V2080B and 1PM2485B indicated that higher densities were found nearer the fault sites. In the case of cables 2V1011B and 1PM2445B the opposite trend was indicated.

TABLE 11
CROSSLINKING DENSITIES OF THE INSULATIONS FROM VARIOUS CABLE SAMPLES

cable	location	footage marker	crosslinking density, %
2V1011B	away from fault	02928	79
2V1011B	near fault	02910	75
1PM2080B	away from fault	00880	71
1PM2080B	near fault	00904	61
1PM2485B	away from fault	00210	81
1PM2485B	near fault	00240	83
1PM2445B	away from fault	00448	74
1PM2445B	near fault	00436	78
79K5-824279-1	random	04582	79
82K5-830040-2	random	00452	68

Table 11 summarizes the crosslinking density measurements of the insulations from those cables that failed during in-situ testing and from the insulations of cable supplied to TVA under contracts 79K5-824279-1 and 82K5-830040-2. Also shown in this table are comparisons between the crosslinking densities of the insulations near and away from the fault sites of the same cables. Overall, the average crosslinking densities for the failed cables are within the range normally expected for this type of insulation and local differences can be explained in terms of the extremes of temperature to which the insulations were exposed.

Infrared spectroscopy was used to analyze the solvent-extracted materials from the insulations that were used for crosslinking density determinations. Figure 28 is an infrared spectrum corresponding to the insulation from cable 2V1011B.

Figures 29 and 30 are infrared spectra corresponding to the insulations from cables 1PM2485B and 1PM2445B, respectively. When compared to Figure 31, a reference spectrum of pure polyethylene, it is apparent that the spectra in Figures 28 through 30 also show only polyethylene present. Spectra obtained from the insulation extractables of cable 1PM2080B were identical to those shown in Figures 28 through 30. Figure 31 is the infrared spectrum obtained from the solvent-extracted materials from the insulation of a cable manufactured under contract 79K5-824279-1. The spectrum from the insulation extractables of a cable manufactured under contract 82K5-830040-2 showed identical characteristics. Overall, the insulations from various vintages showed identical chemical characteristics and no anomalous ingredients were found near the fault sites of those cables that failed during testing.

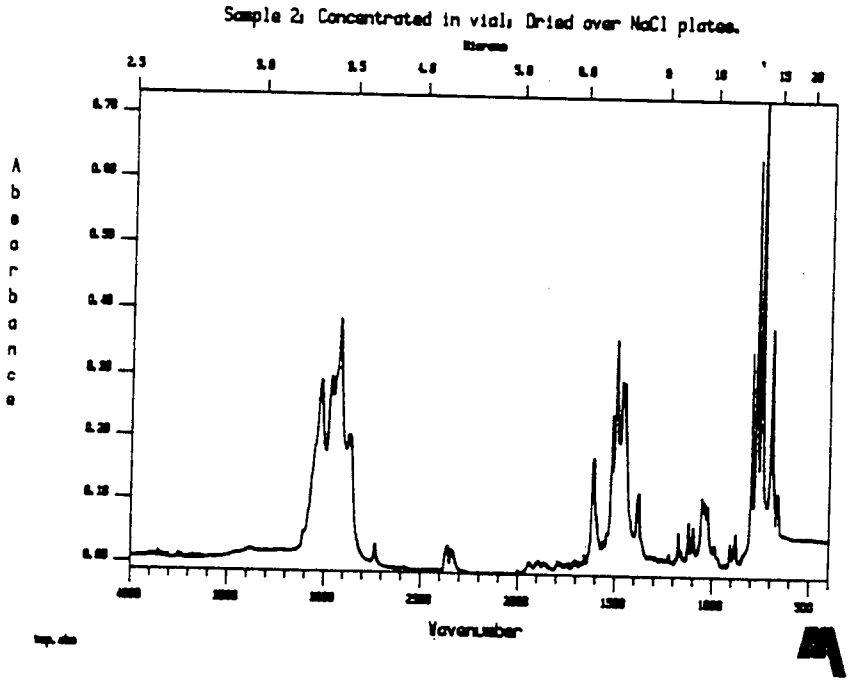

Figure 28. Infrared Spectrum of Solvent-Extracted Materials from the Insulation of Cable 2V1011B

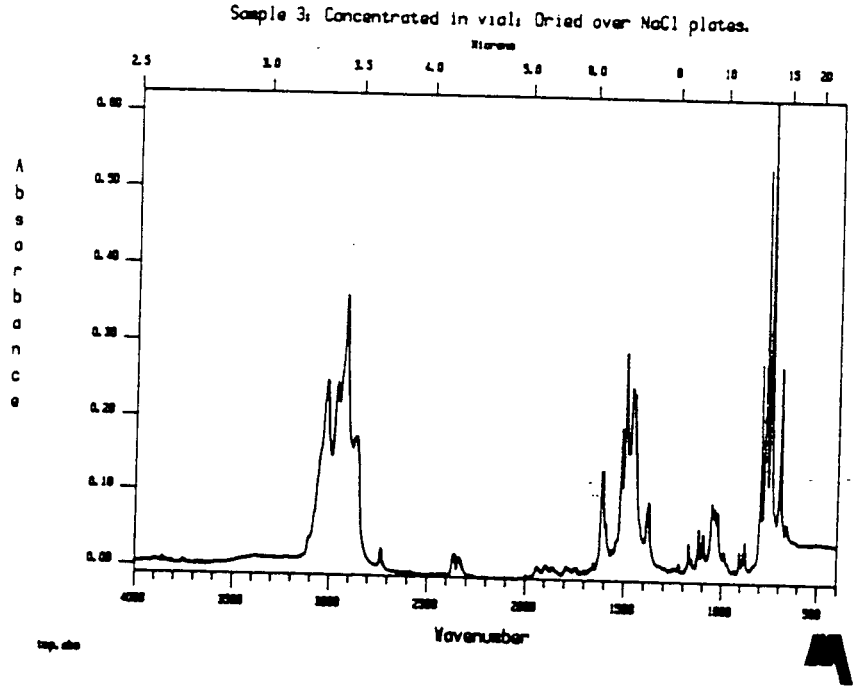

Figure 29. Infrared Spectrum of Solvent-Extracted Materials from the Insulation of Cable 1PM2485B

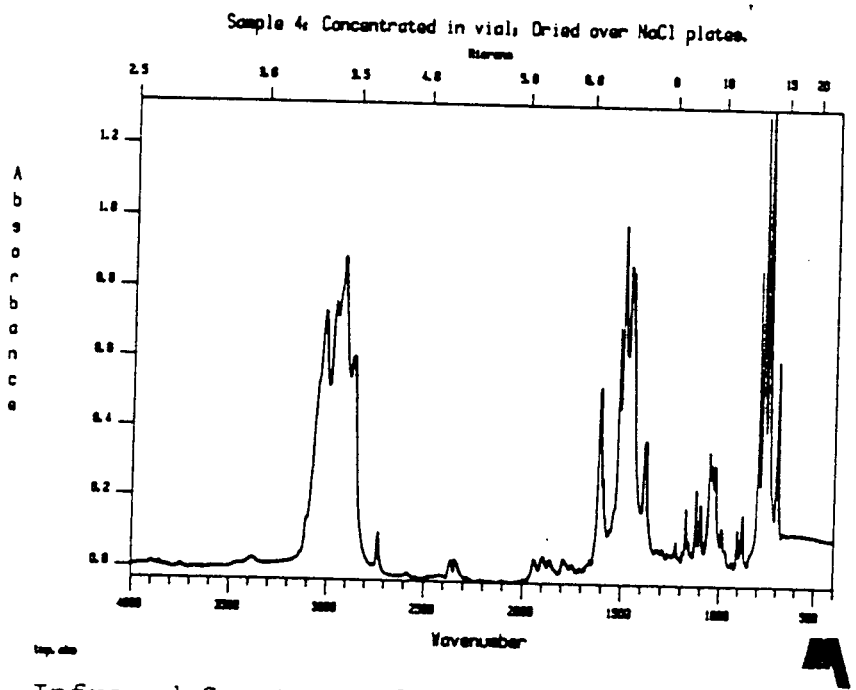

Figure 30. Infrared Spectrum of Solvent-Extracted Materials from the Insulation of Cable 1PM2445B

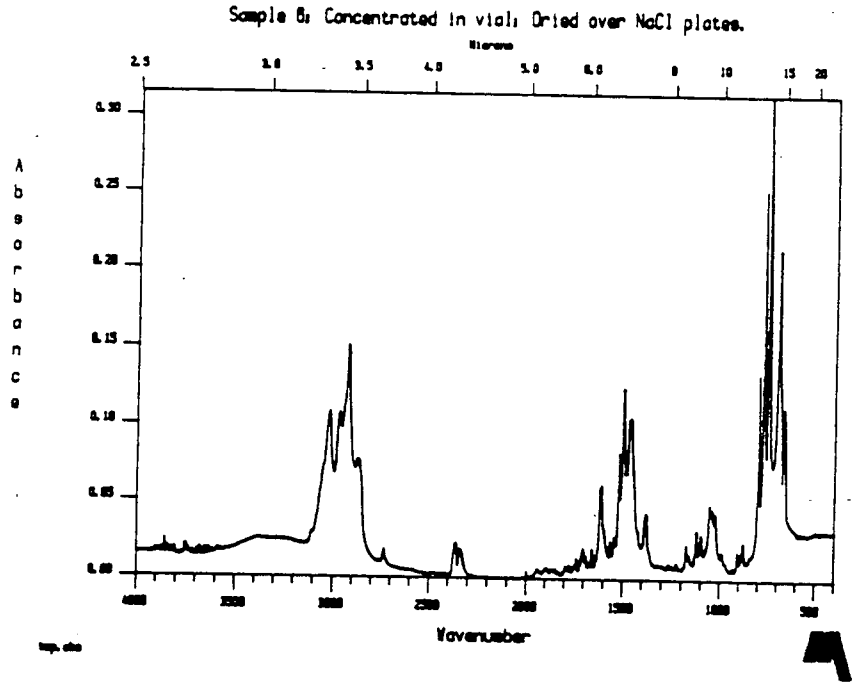

Figure 31. Infrared Spectrum of Solvent-Extracted Materials from Reference Specimen of Pure Polyethylene

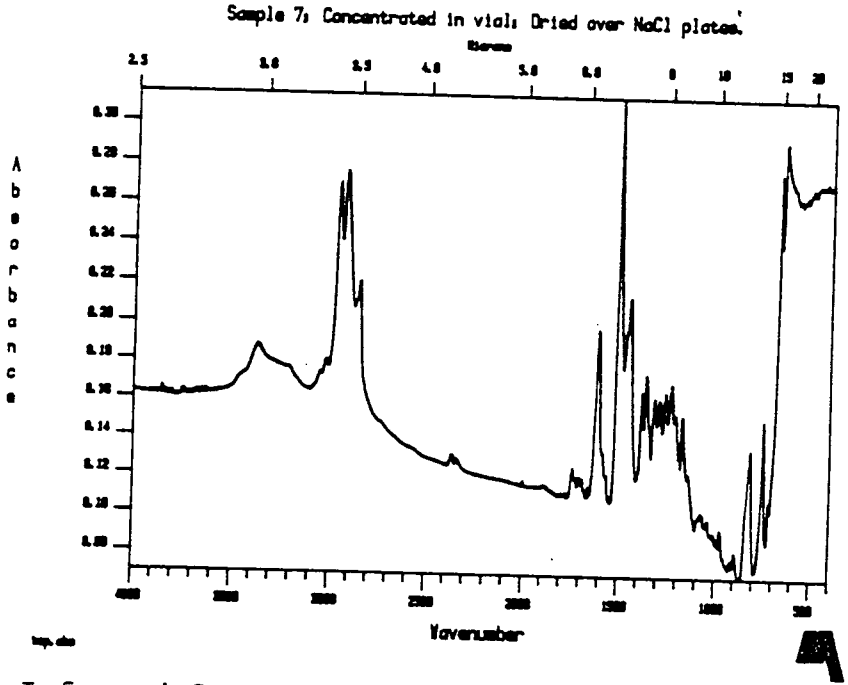

Figure 32. Infrared Spectrum of Solvent-Extracted Materials from Insulation of Cable Provided to TVA Under Contract 79K5-824279-1

Thermogravimetric analysis of the insulations from the cables that failed during in-situ testing exhibited the weight loss vs. temperature characteristics shown in Figure 33 corresponding to cable 2V1011B, near the fault site. Figure 34 is a thermogram for the insulation of this cable away from the fault site. The two thermograms compare point-to-point with a high degree of correlation. Figure 35 shows the weight loss vs. temperature characteristics for the insulation of cable 1PM2445B near the fault site. The TGA scan for this cable away from the fault site is shown in Figure 36. The TGA scans for the insulations of cables 1PM2485B and 1PM2080B were almost identical to those shown in Figures 33 through 36, whether near or away from the fault sites. Figures 37 and 38 show the weight loss vs. temperature characteristics for the insulations of cables supplied under contacts 79K5-824279-1 and 82K5-830040-2, respectively. These results indicate that there are no detectable formulation differences between the various vintages of cable insulations and that no formulation anomalies are associated with the fault areas of the cables that failed during in-situ testing.

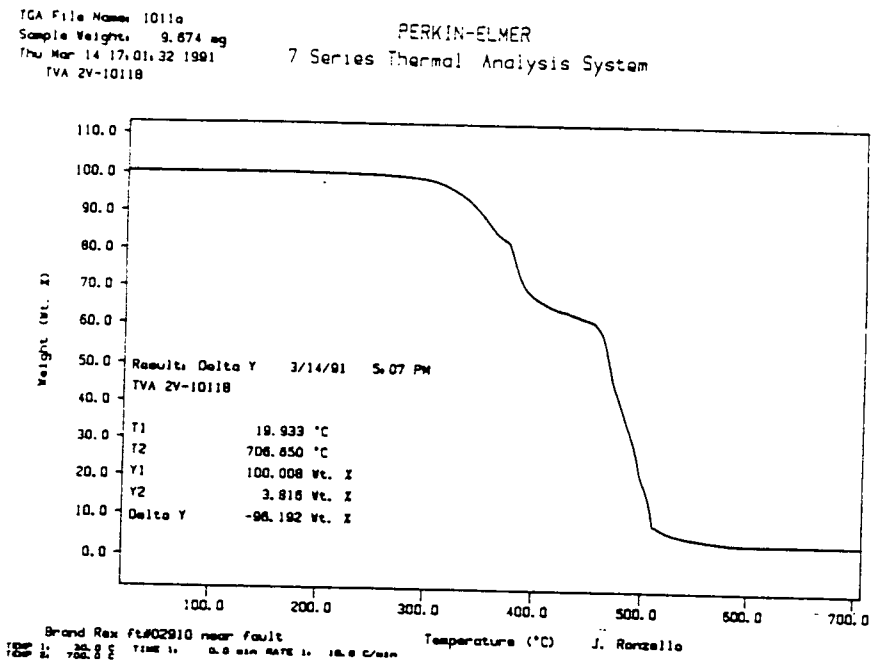

Figure 33. TGA Scan Showing Weight Loss vs. Temperature Characteristics of the Insulation from Cable 2V1011B, Near the Fault Site

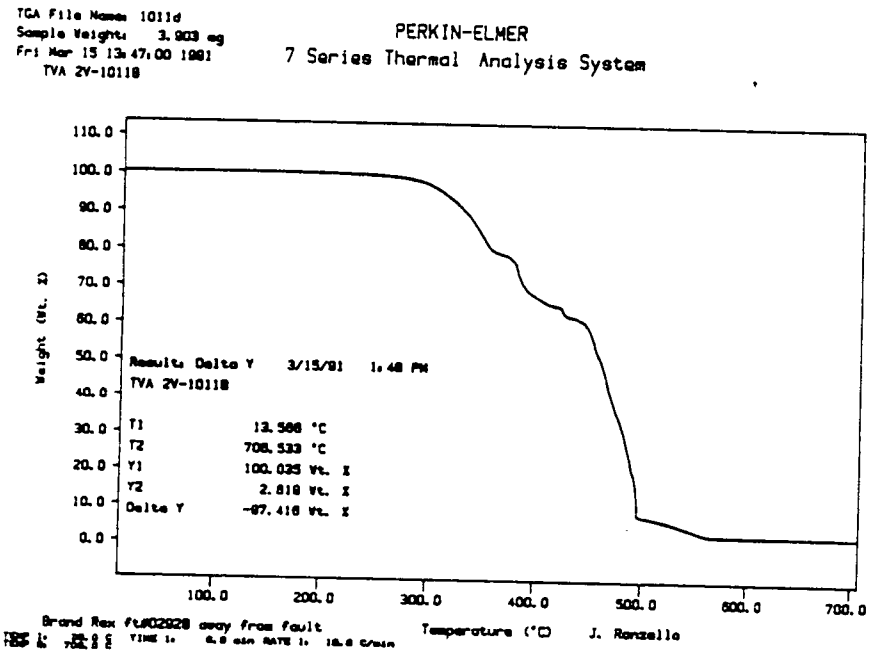

Figure 34. TGA Scan Showing Weight Loss vs. Temperature Characteristics of the Insulation from Cable 2V1011B, Away from the Fault Site

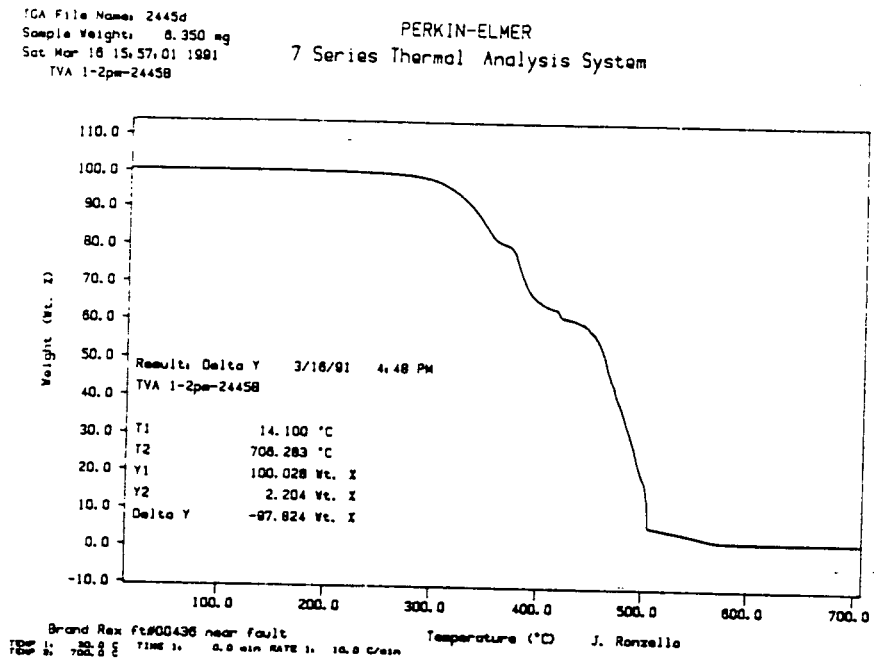

Figure 35. TGA Scan Showing Weight Loss vs. Temperature Characteristics of the Insulation from Cable 1PM2445B, Near the Fault Site

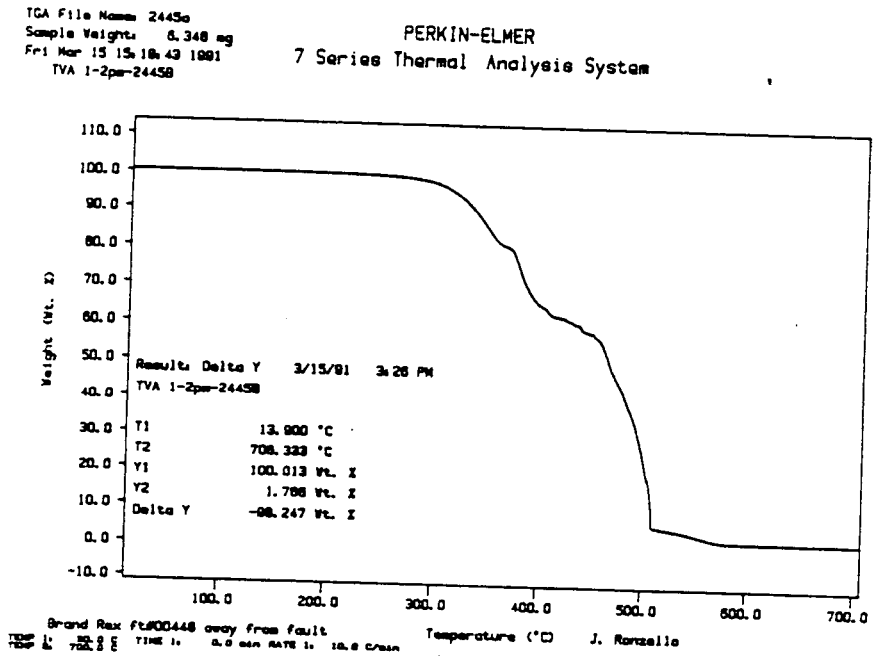

Figure 36. TGA Scan Showing Weight Loss vs. Temperature Characteristics of the Insulation from Cable 1PM2445B, Away from the Fault Site

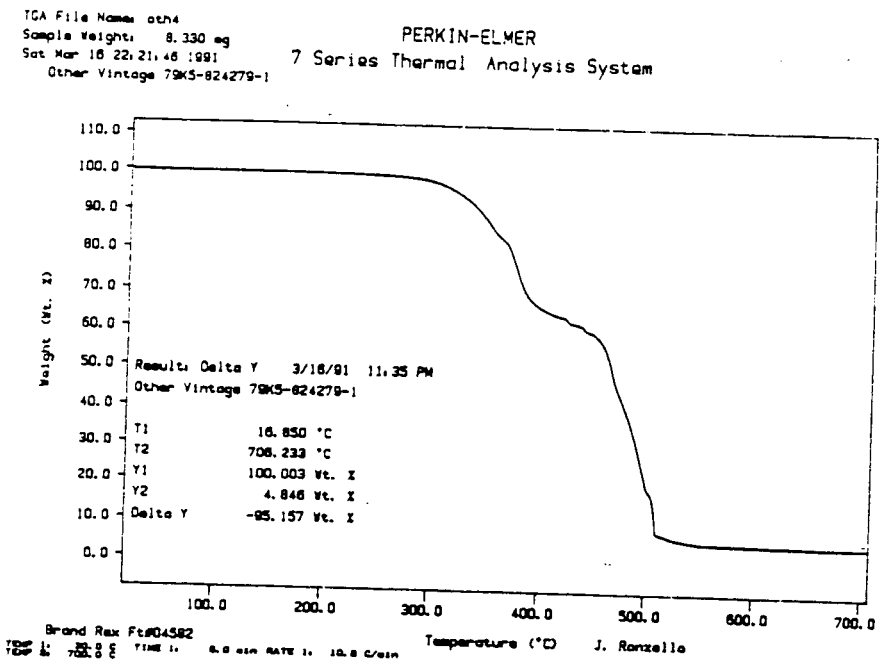

Figure 37. TGA Scan Showing Weight Loss vs. Temperature Characteristics of the Insulation from Cable Supplied Under Contract 79K5-824279-1

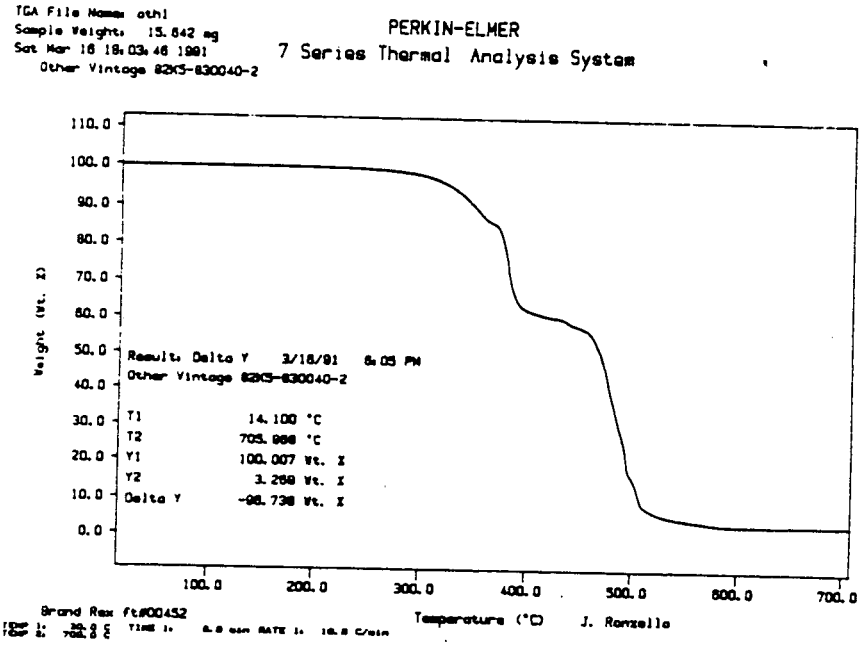

Figure 38. TGA Scan Showing Weight Loss vs. Temperature Characteristics of the Insulation from Cable Supplied Under Contract 82K5-830040-2

TGA scans were obtained at closely-spaced incremental locations along the length of cable 1PM2485B to assess whether significant variations in the local concentration of inorganic components could be detected. Figures 39, 40, and 41 are TGA scans corresponding to three locations near the fault site of this cable. Figure 39 shows the insulation characteristics nearest the fault site. Figures 40 and 41 correspond to locations 1.0 in. and 1.5 in. away from the fault site, respectively. When these figures are compared, no differences are indicated in the insulation formulation along the length of the cable near the fault site.

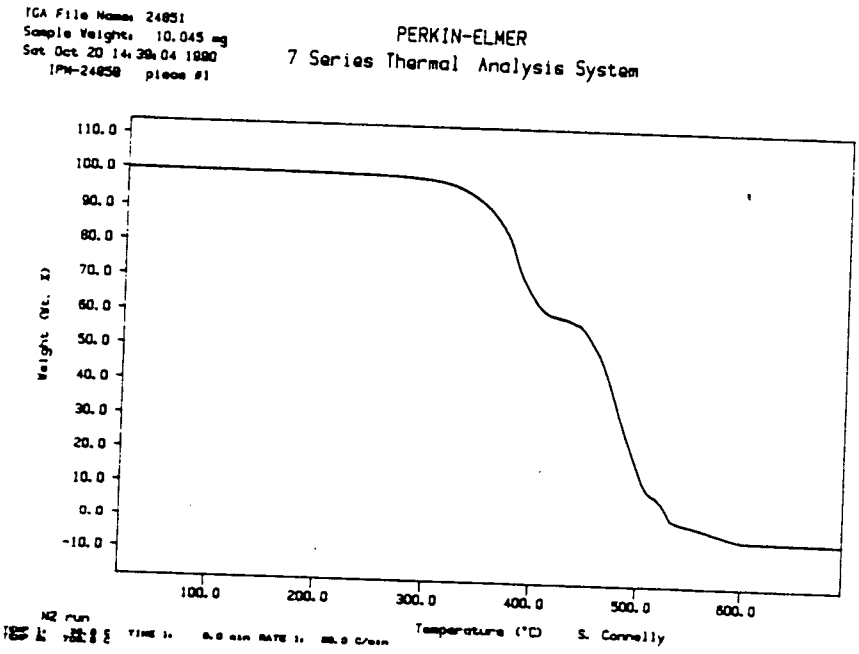

Figure 39. TGA Scan of the Insulation Compound within 0.5 in. of the Fault Site of Cable 1PM2485B

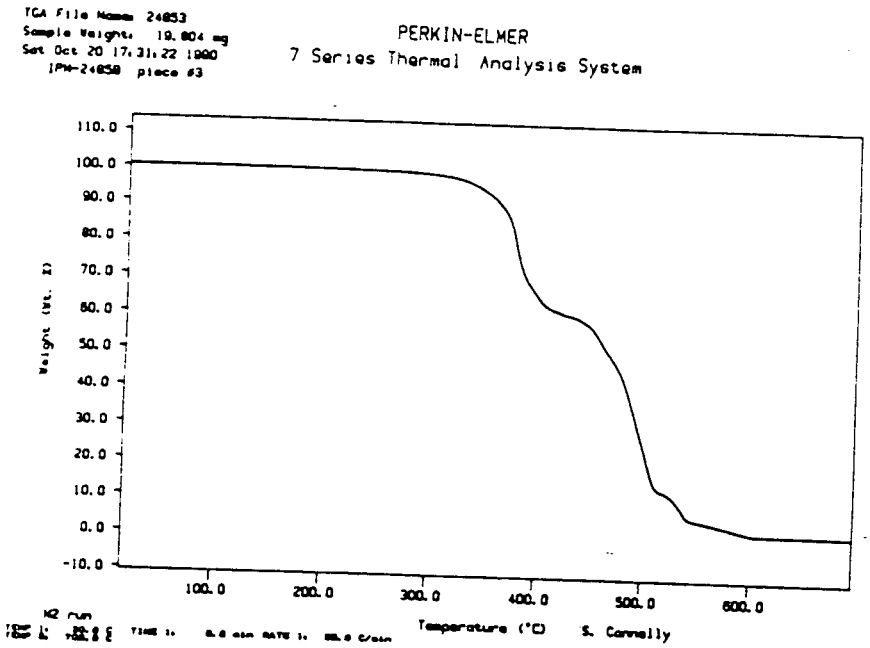

Figure 40. TGA Scan of the Insulation Compound within 1.0 in. of the Fault Site of Cable 1PM2485B

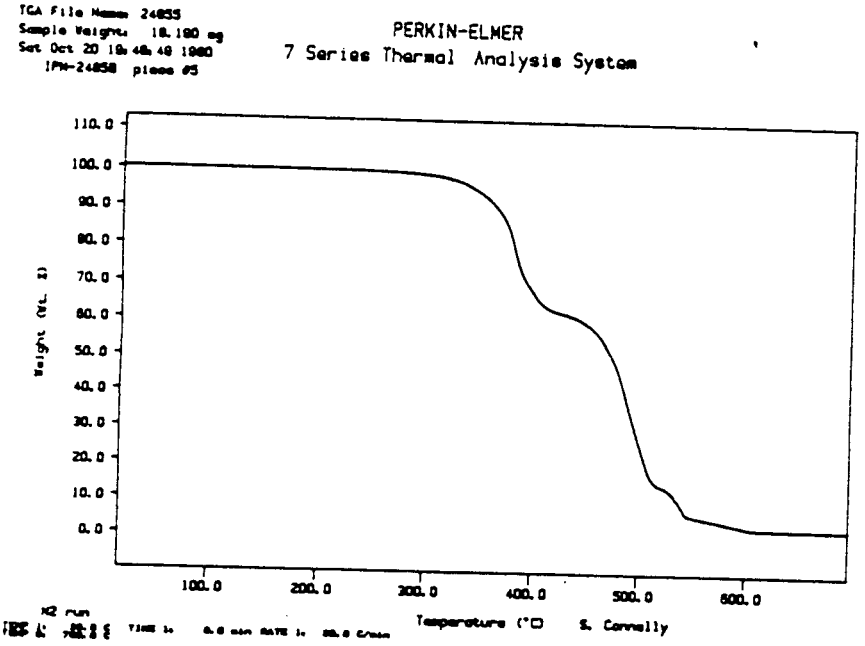

Figure 41. TGA Scan of the Insulation Compound within 1.5 in. of the Fault Site of Cable 1PM2485B

The insulation morphologies of cable that failed during in-situ testing were compared with cables supplied under contracts 79K5-824279-1 and 82K5-830040-2. While it was noted earlier in this report that atypically large particles of silica and antimony trioxide were found at the fault sites of the affected cables, the insulations of these cables were examined to determine if these particles were generally present or uniquely associated with the fault sites. Figure 42 shows a representative cross-section of the insulation from cable supplied under contract 79K5-824279-1. The inorganic particles can be seen to be consistent in their physical dimensions and uniformly distributed. Figure 43 presents a representative view of the insulation from a cable supplied under contract 82K5-830040-2. As in the previous case, the inorganic particles are uniform in size and uniformly distributed. Approximately 20 such sections were examined from various locations along the lengths of these cables and the areas shown in Figures 42 and 43 were determined to be representative. Figure 44 shows the morphology of the insulation from cable 2V1011B, near the fault site. In this Figure, several large particles of inorganic material can be seen within the insulation. Similarly, Figure 45 is a representative view of the insulation from cable 1PM2445B, near the fault site. Figure 46 shows the insulation from this cable, but from a location approximately 4 in. away from the fault site. In this view, the large particles of inorganic material are not evident.

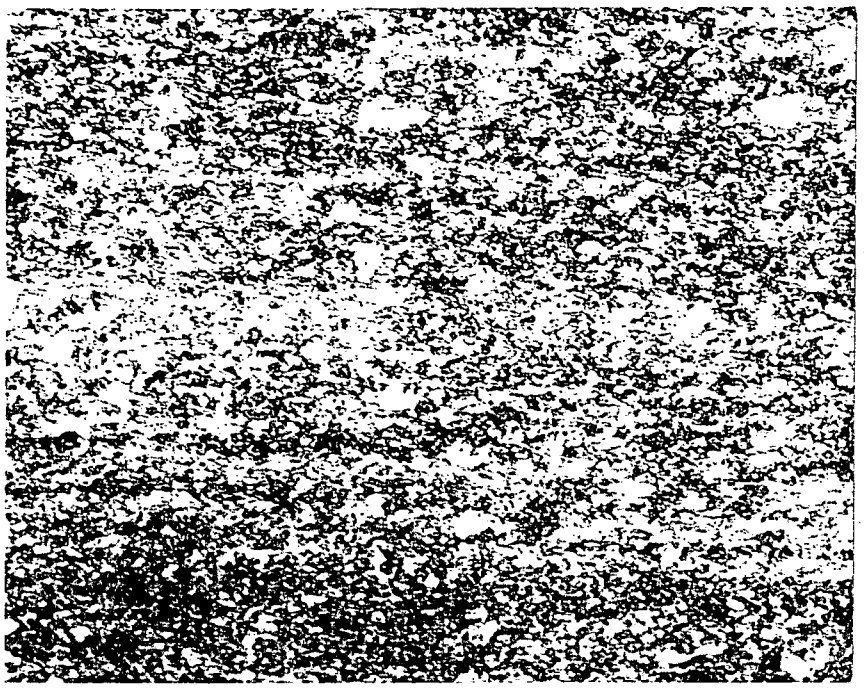

Figure 42. Thin Section of the Insulation, Viewed with Transmitted Illumination, from Cable Supplied Under Contract 79K5-824279-1, 100x Magnification

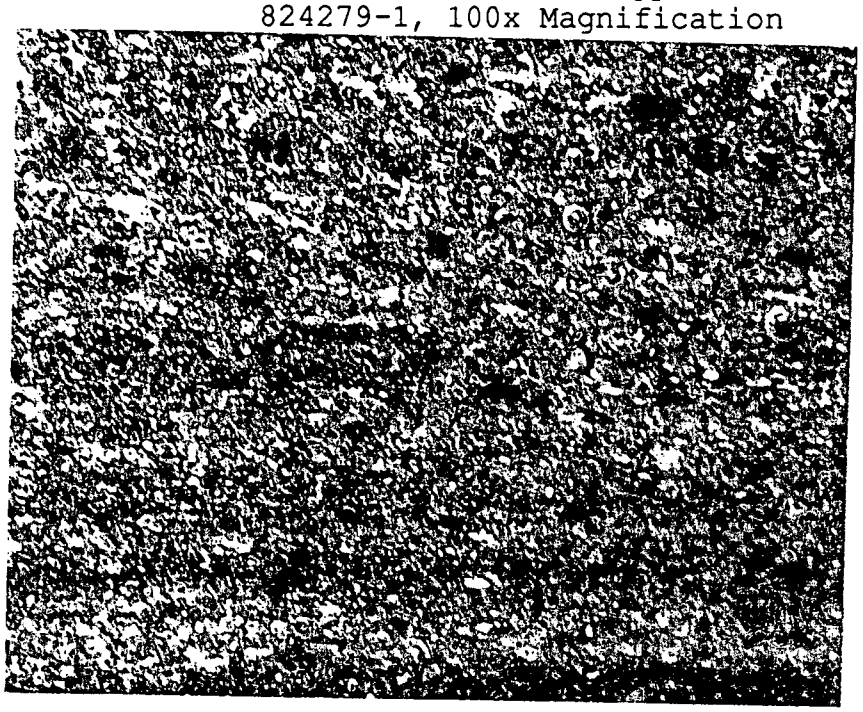

Figure 43. Thin Section of the Insulation, Viewed with Transmitted Illumination, from Cable Supplied Under Contract 82K5-830040-2, 100x Magnification

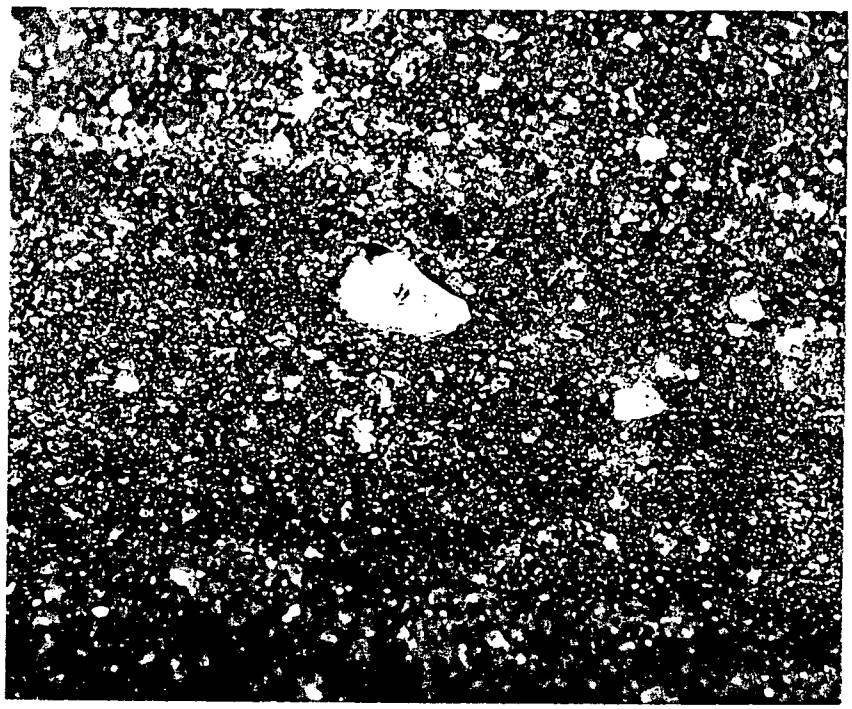

Figure 44. Representative View of a Thin Section of the Insulation from Cable 2V1011B, Near the Fault Site, Shown with Transmitted Illumination, 100x Magnification

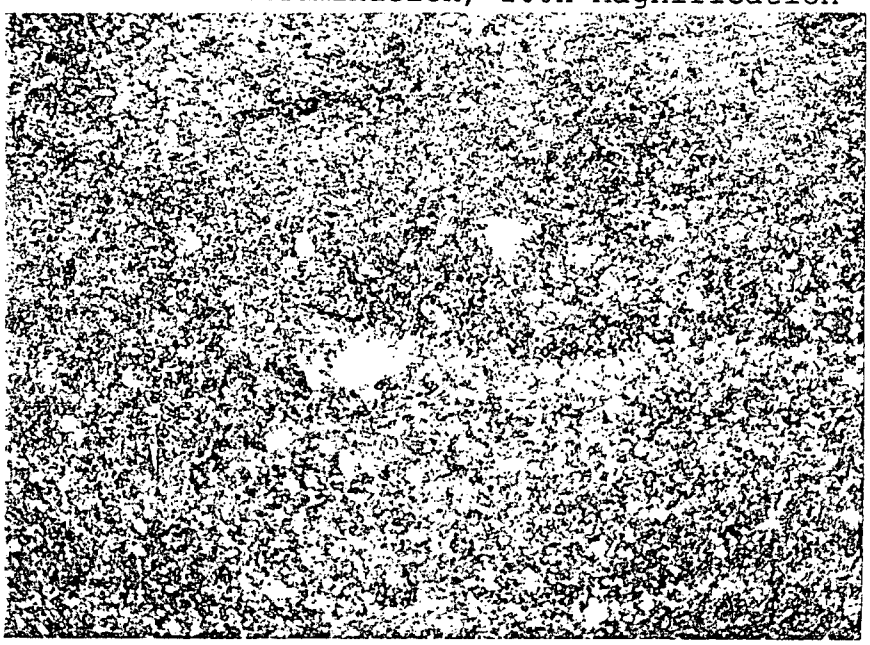

Figure 45. Representative View of a Thin Section of the Insulation from Cable 1PM2445B, Near the Fault Site, Shown with Transmitted Illumination, 100x Magnification

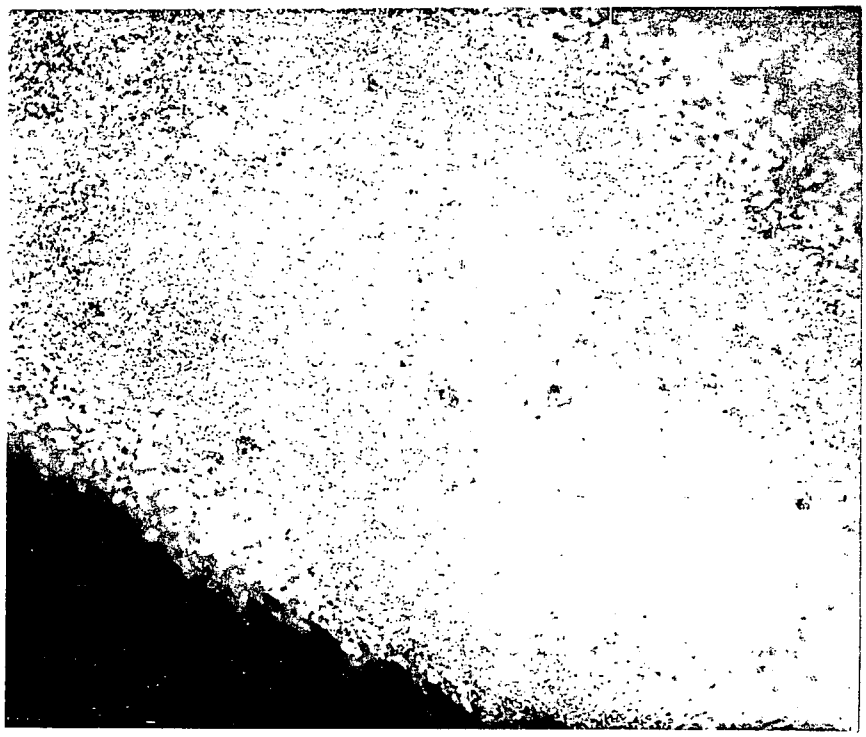

Figure 46. Representative View of a Thin Section of the Insulation from Cable 1PM2445B, Away from the Fault Site, Shown with Transmitted Illumination, 100x Magnification

Comparison between the size and size distributions of the inorganic constituents within the insulations of the cables is somewhat subjective when photographic information alone is used, such as that presented in Figures 42 through 46. Computerized image analysis was used to provide a quantitative basis for comparing the size of the inorganic components between cables from various vintages and to compare these measurements near and away from the fault sites of representative specimens. For this application, the insulations were subjected to plasma etching to isolate the inorganic particles from the organic components of the insulation. Sections 0.75 in. long from cables supplied under contracts 79K5-824279-1 and 82K5-830040-2 were subjected to plasma etching for approximately 6 hours. The etched sections were then

ultrasonically agitated in 10 ml ethyl alcohol. The cable sections were then returned to the plasma etcher for another 4 hours, then treated in the alcohol again. In this manner, the inorganic components of the insulations were completely separated. An identical procedure was used to prepare the insulations from cables 2V1011B and 1PM2445B. Areas near the fault sites were compared with areas on the same cables approximately 6 in. away from the fault sites. In Figure 47, the particle size distributions for an area of the insulation from cable 2V1011B, 6 in. away from the fault, are compared to particle size distributions from cable supplied to TVA under contracts 79K5-824279-1 and 82K5-830040-2. From these data, it is indicated that the insulation from the failed cable contains larger inorganic particles within the insulation than were found in either of the other vintage cables. This difference is shown more clearly in an expanded view of the particle size distributions, as shown in Figure 48. The two non-failed vintage cables compare quite closely with respect to their inorganic particle size distributions. Figure 49 compares the inorganic component particle size distributions for the insulation of cable 2V1011B near and away from the fault site. Figure 50 presents the same data shown in Figure 49, but with an expanded particle size scale. From these data, it appears that there are larger particles concentrated near the fault site than were found at an area remotely located.

Similar measurements of the inorganic components from the insulation of cable 1PM2445B. Figure 51 compares the particle size distributions of the inorganic components of cable 1PM2445B to the insulations of cable provided under contracts 79K5-824279-1 and 82K5-830040-02. Figure 52 presents the same data on an

expanded scale to more clearly demonstrate the measured differences.

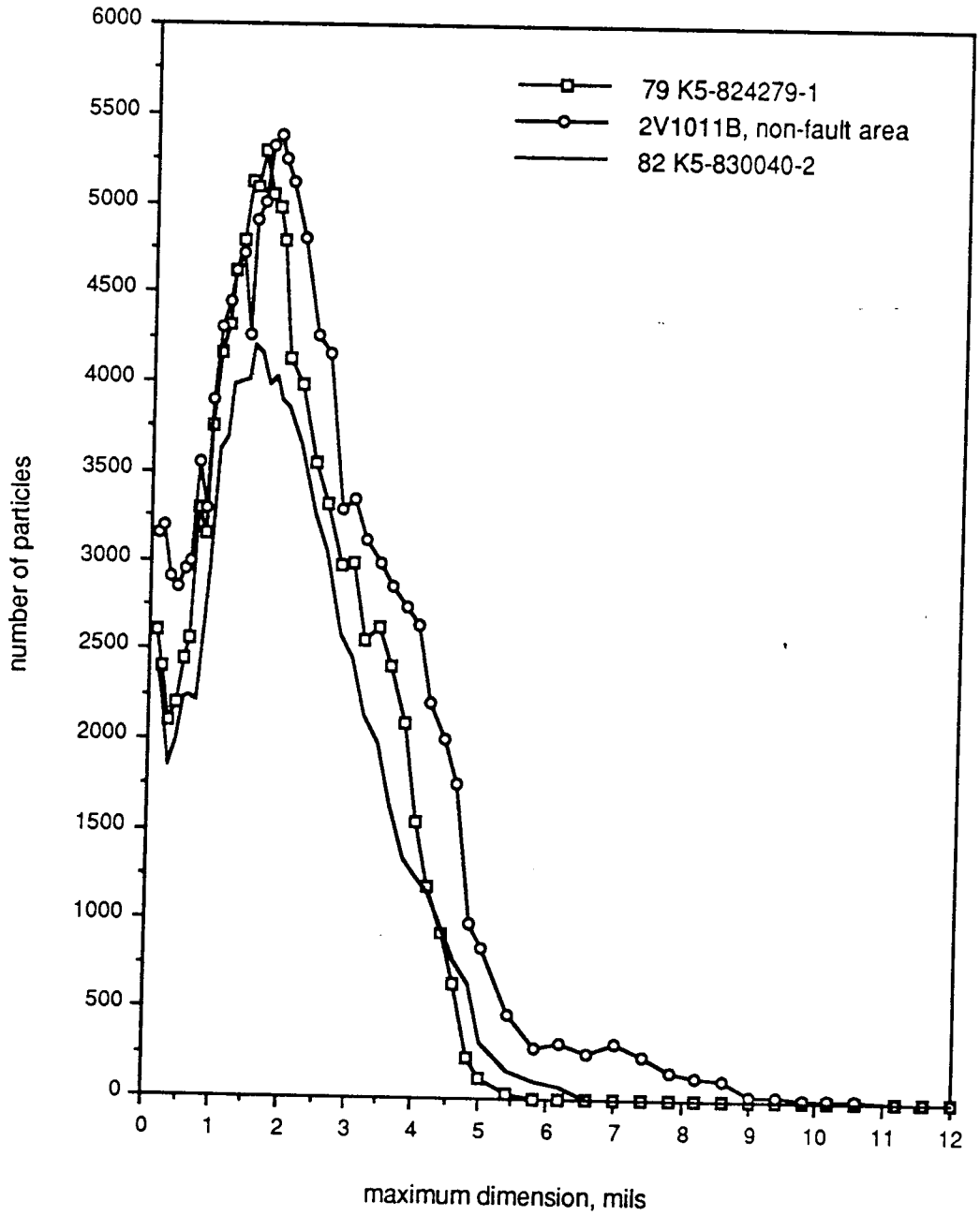

Figure 47. Size Distributions of Plasma-Extracted Inorganic Components of the Insulations, Comparing Failed Cable 2V1011B to Non-Failed Vintages

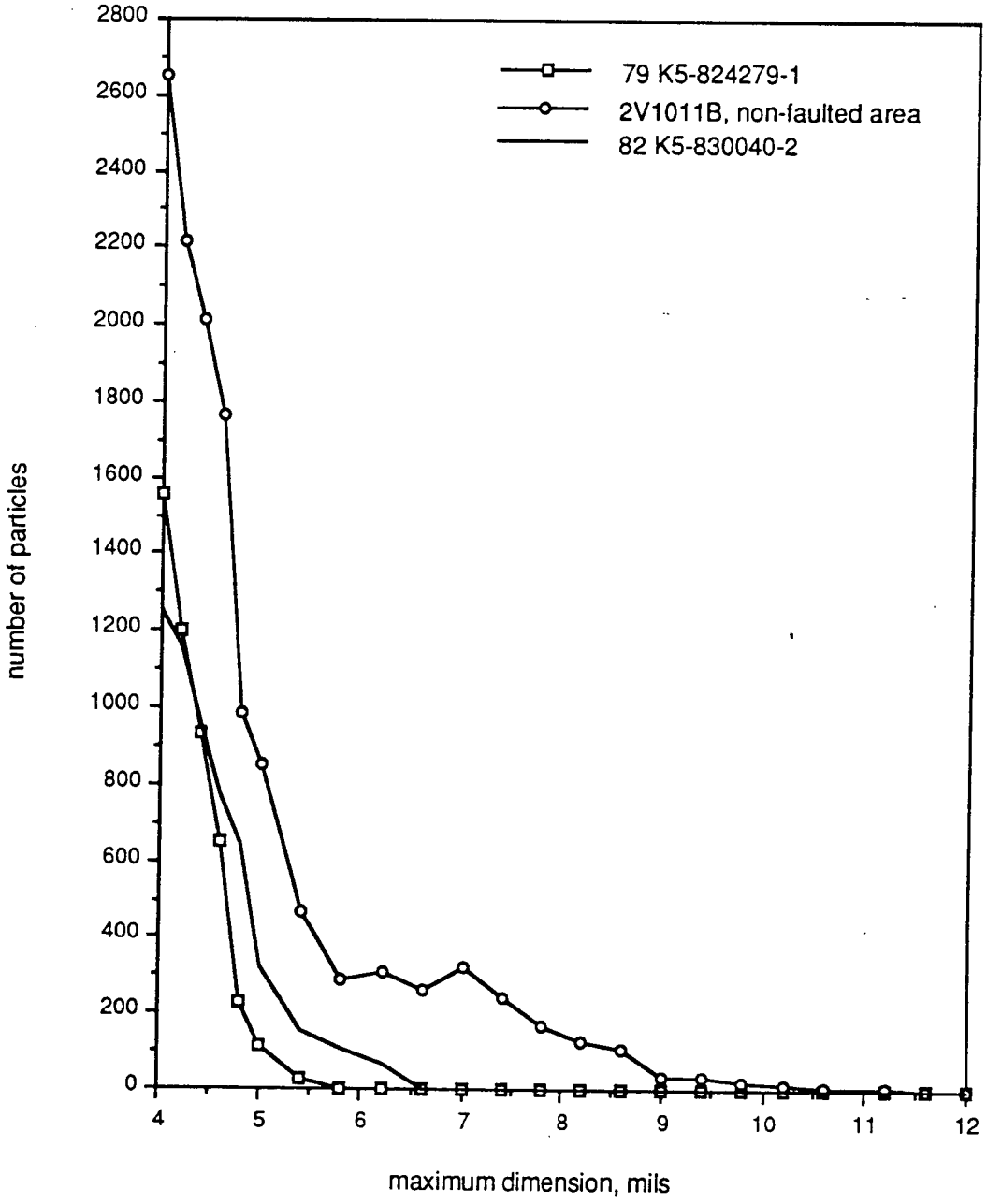

Figure 48. Size Distributions of Plasma-Extracted Inorganic Components of the Insulations, Comparing Failed Cable 2V1011B to Non-Failed Vintages (Expanded Scale)

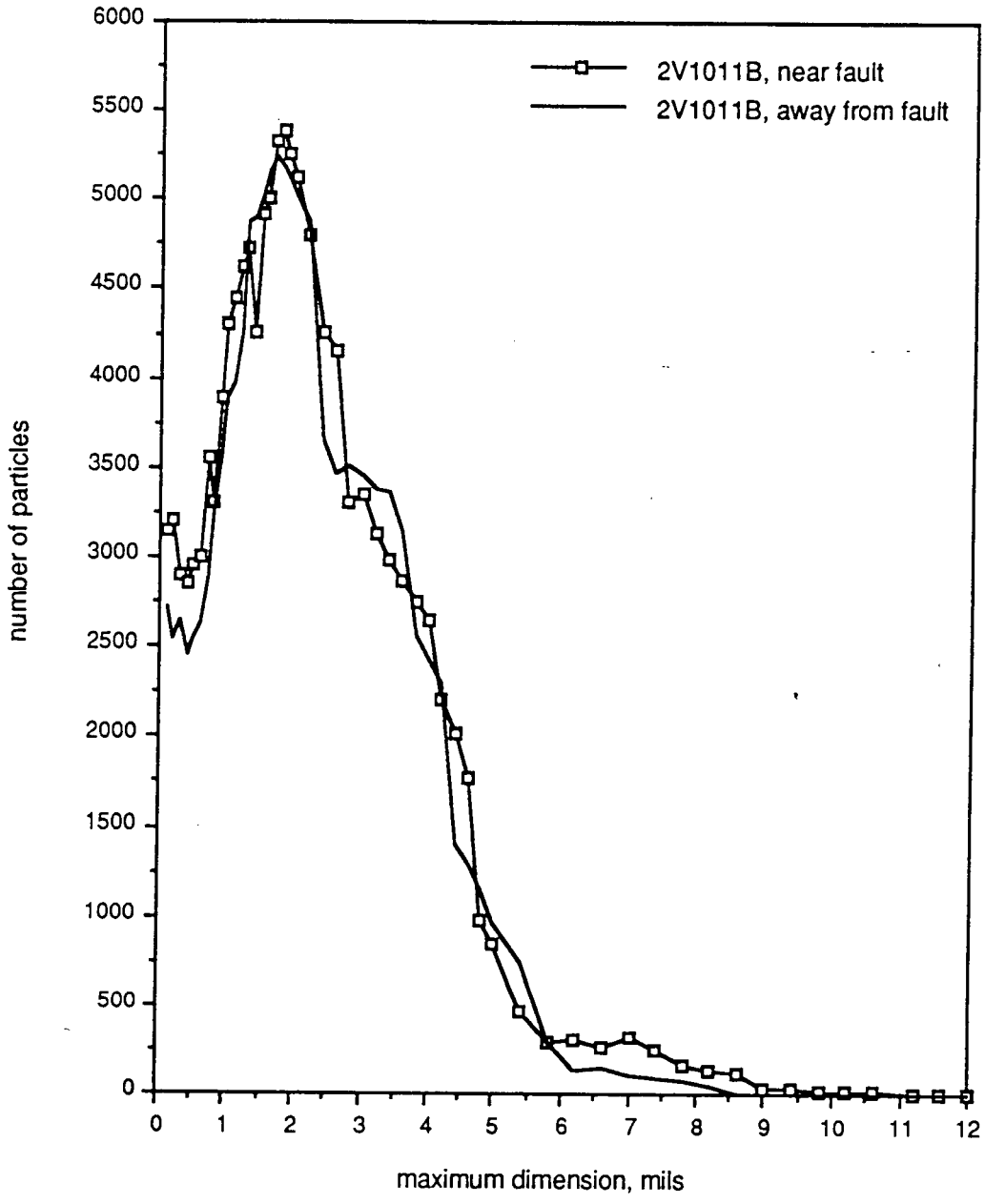

Figure 49. Size Distributions of Plasma-Extracted Inorganic Components of the Insulation of Cable 2V1011B Comparing Failed to Non-Failed Locations

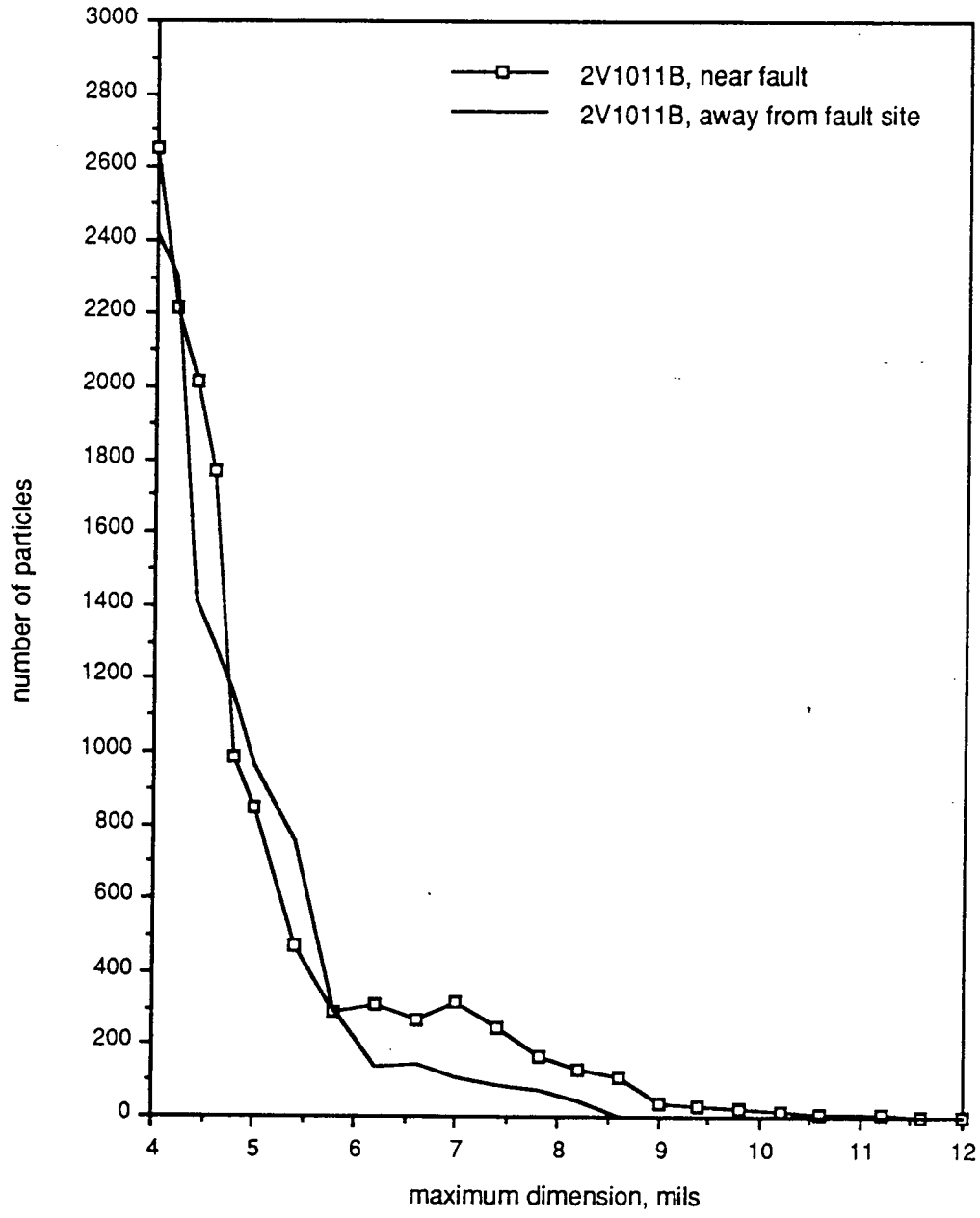

Figure 50. Size Distributions of Plasma-Extracted Inorganic Components of the Insulation of Cable 2V1011B Comparing Failed to Non-Failed Locations (Expanded Scale)

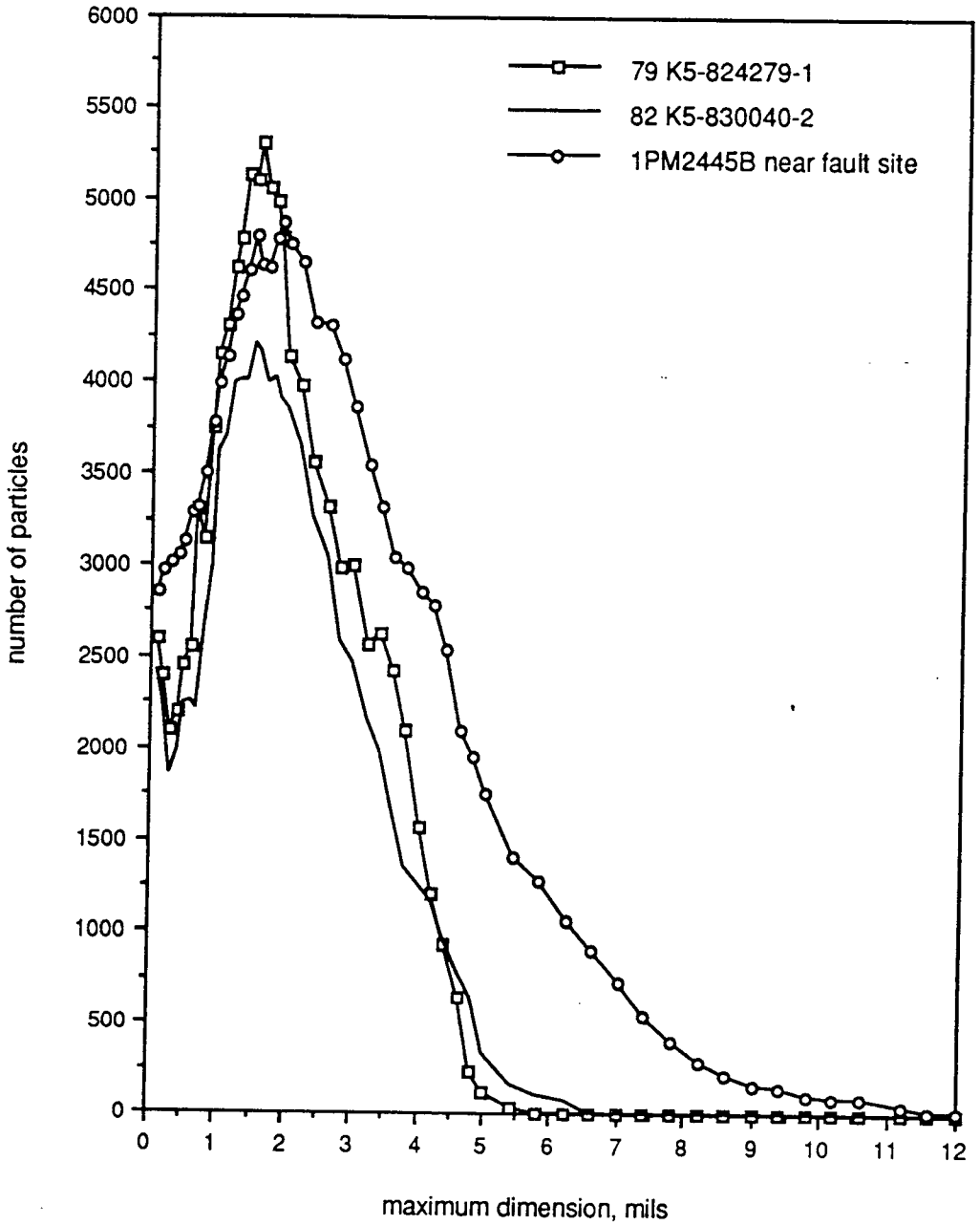

Figure 51. Size Distributions of Plasma-Extracted Inorganic Components of the Insulations, Comparing Failed Cable 1PM2445B to Non-Failed Vintages

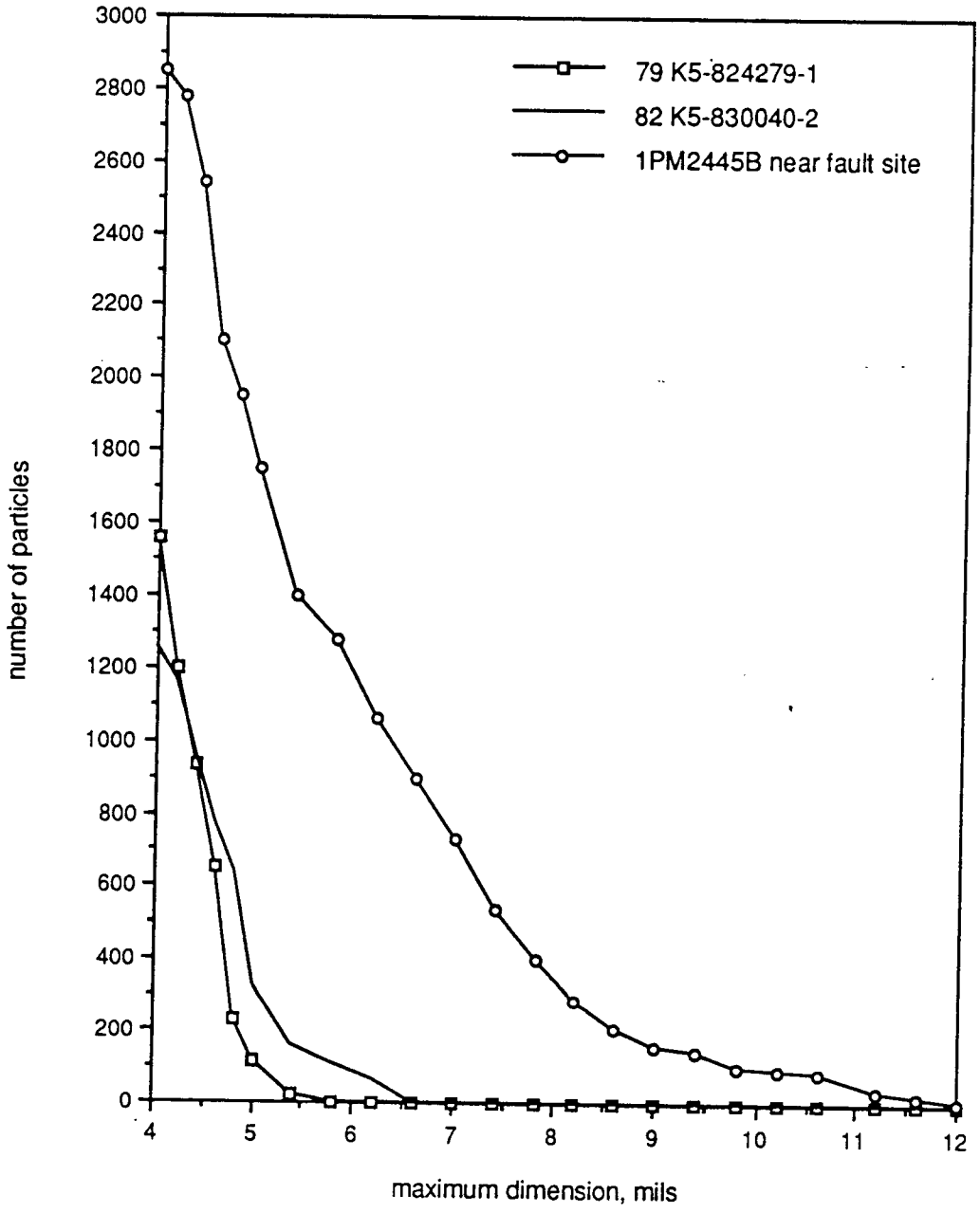

Figure 52. Size Distributions of Plasma-Extracted Inorganic Components of the Insulations, Comparing Failed Cable 1PM2445B to Non-Failed Vintages (Expanded Scale)

5.8 Analysis of 80K6-825419 Cables Following LOCA Testing

5.8.1 Introduction

Following the analyses that indicated an association between abnormally large inorganic particles at the fault sites of the cables supplied under contract 80K6-825419, TVA subjected to LOCA testing samples of this cable, obtained from cables removed from WBN or from warehoused reels. All samples were found to pass the LOCA testing protocol. Following this test program, the cables were subjected to dc high voltage testing to determine if any faults would occur and, if they did occur, to determine the reasons for their occurrence at specific sites.

Four cables failed during dc testing after the LOCA aging. These are indicated in Table 12. Since the insulations from these cables had been degraded by the LOCA aging conditions, testing of the nominal properties of the insulations, such as tensile strength, elongation limit, density, crosslinking density, shrink-back, and analysis of solvent-extractables was not conducted. Instead, the insulations at the fault sites were analyzed for wall thickness, concentricity, and morphology.

TABLE 12
BREAKDOWN VOLTAGES OF CABLES SUBJECTED TO LOCA TESTING

cable	mfr. reel	location	breakdown, Vdc
01-A-2	1-74546	warehouse	4800
03-A-2	1-74546	warehouse	4000
35-A-2	1-000795	installed/2V1131B	4800
36-A-2	1-000795	installed/2V1131B	3800

5.8.2 Analysis Procedures

The cables indicated in Table 12 were cut into sections approximately 5 in. long, with the fault sites centrally located. Following the protocol shown in Figure 53, sections near and including the fault sites were prepared for analysis. Insulation wall thicknesses were measured using a calibrated eyepiece scale and an optical microscope.

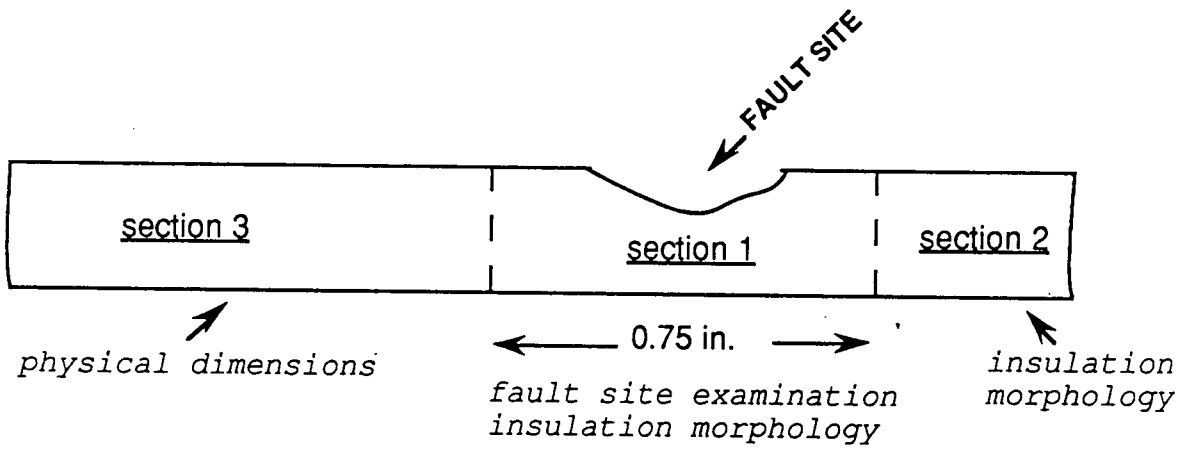

Figure 53. Protocol for Sectioning and Analysis of Fault Sites from Post-LOCA Test Failures

The fault sites were examined with a stereomicroscope using a magnification range of 2 through 40x. These sites were examined for anomalies in their materials, visible manufacturing defects, mechanical damage, or other factors that may have contributed to or caused the failures.

Insulation sections near the fault sites of the LOCA tested cables were prepared with a microtome (sections 1 and 2 as shown in Figure 53). Slices approximately 1 mil thick were obtained

from each of the four cables. These were then examined using a polarizing microscope with either transmitted or reflected illumination and magnifications ranging from 40x through 200x. Photographic records were prepared during these observations and are presented in this report.

The insulation wall thicknesses were measured using a microscope. These measurements were made with a calibrated eyepiece scale which was tested with a NIST-certified standard scale having a resolution of 0.1 μm. Cross-sections of the insulation were prepared with a microtome for these measurements. The wall thicknesses were measured at a location within 1 in. of the fault sites of each of the four cables, as shown in Figure 53.

To examine the particle size of the inorganic components of the insulations of the cables, plasma etching was again used. In this case, the insulation had become embrittled by the LOCA testing conditions, so it could not be cut away from the cable without endangering its integrity. Sections of the cables approximately 0.75 in. long, with the fault sites centrally located, were subjected to plasma etching. This required treatment times in excess of 12 hours. At intervals ranging from approximately 2 hours to 6 hours, the sections of cable were removed from the etching system and immersed in approximately 10 ml of ethyl alcohol in a clean, covered glass container. This was then ultrasonically agitated to remove the inorganic particulates from the cable surfaces. Following this treatment, the cables were returned to the etching system to remove more of the organic material. This process was repeated until the insulations were completely removed from the cables. The inorganic components of

the insulations contained within the ethyl alcohol were stored for subsequent examination and measurement with the microscope.

Following complete removal of the insulations from the fault sites of the four cables, the fault sites were examined with a stereomicroscope to determine if any anomalies were present at these locations. Protrusions, nicks, broken strands, etc. could act as electrical stress concentrators, thus explaining the localized nature of the faults that were experienced.

The dispersions of the plasma-separated inorganic components were examined using a polarizing microscope, as previously used to examine the inorganic components from the fault areas of the cables that failed during in-situ electrical testing. The dispersions were first agitated ultrasonically then a small amount was removed with a pipette and placed on a glass microscope slide. These were then encapsulated with a resin and examined with the microscope. Magnifications ranging from 40x through 200x were used to examine and measure the inorganic particles. Computerized image analysis was also used to obtain particle size distributions from selected cables samples.

5.8.3 Results

The fault sites of cables 01-A-2, 03-A-2, 35-A-2, and 36-A-2 were examined with the aid of a stereomicroscope. No mechanical damage or construction anomalies could be found at any of the fault sites. No apparent voids or other materials defects were found.

The insulation wall thicknesses of the cables that failed hipot testing after LOCA simulation were measured. These values are summarized in Table 13. Some of the dimensions were found to be outside the TVA specified minimum insulation wall thickness of 27 mils. It should be noted that the insulation wall thicknesses of the cables shown in Table 13 appear somewhat lower, overall, than those shown in Table 6. This is attributed to the effect of LOCA testing on the materials. The values of insulation wall thickness following LOCA testing may not be representative of the conditions preceding these tests.

TABLE 13
INSULATION WALL THICKNESSES OF CABLES FOLLOWING LOCA TESTING

cable	minimum wall thickness, mils	maximum wall thickness, mils
01-A-2	26.6	28.1
03-A-2	26.6	27.9
35-A-2	26.5	27.4
36-A-2	26.6	27.4

Microscopic examination of thin sections of the insulation obtained from near the fault sites of the four cables revealed that a number of large particles were present in the insulation that were not found in the insulations of cable supplied to TVA under contracts 79K5-824279-1 and 82K5-830040-2. Figures 54 and 55 show representative views of the insulations from cables 35-A-2 and 03-A-2, respectively. Several large particles can be seen in these photographs. At the bottom of each photograph is a 10 mil scale. Comparison of this scale to the dimensions of some of the particles shown in Figures 54 and 55 indicates that particles are present in excess of 10 mils in their longest dimension.

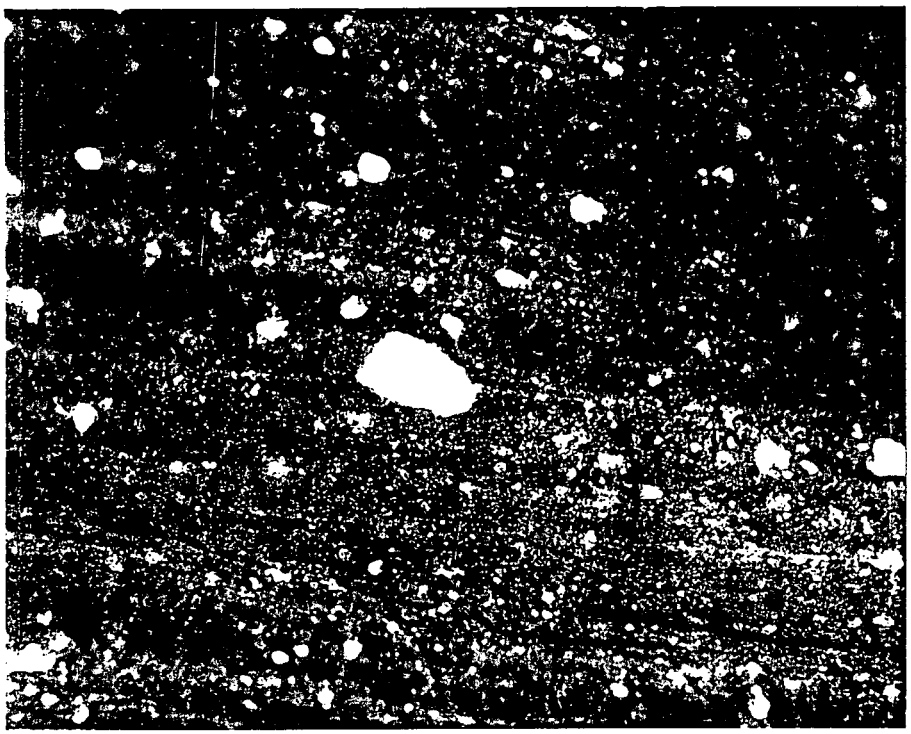

Figure 54. Microtomed Sections of Insulation from Cable 35-A-2, Showing Large Inorganic Particles, 100x Magnification

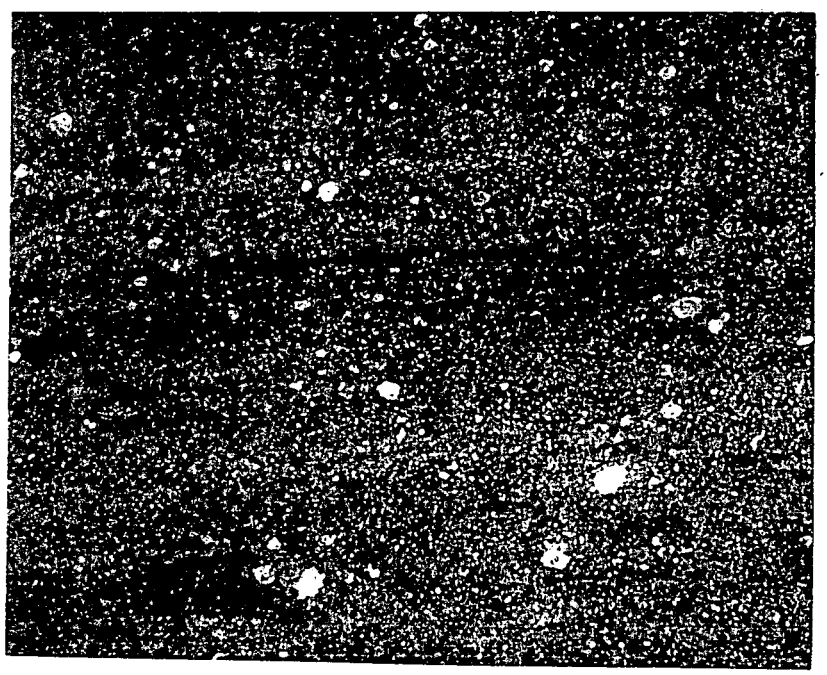

Figure 55. Microtomed Sections of Insulation from Cable 03-A-2, Showing Large Inorganic Particles, 100x Magnification

Size distributions of the inorganic components of the insulations were determined for cable 35-A-2 using computerized image analysis. Figure 56 compares the particle size distributions for cables supplied under contracts 79K5-824279-1 and 82K5-830040-2 to that from cable 35-A-2. These data indicate that there are considerably more large particles of inorganic materials in the insulations of the cable that failed electrical tests following LOCA aging. The differences between these vintages are shown in more detail in Figure 57. In Figures 56 and 57, the maximum displayed particle length is 12 mils. In fact, particles larger than this were found within the insulations of cables 01-A-2, 03-A-2, 35-A-2, and 36-A-2. Since there were only a few of these particles present, they would not have been resolved on the scales used to display the particle size distributions.

The polarizing microscope was used to inspect the plasma-extracted inorganic particles from the insulations of the LOCA-tested cables. This disclosed a number of large particles, such as those shown in Figures 58 and 59, from the insulation of cable 35-A-2. The particle shown in Figure 58 has a maximum dimension of 14 mils and that in Figure 59 is approximately 15 mils. Figure 60 shows one of the large particles found in the plasma-extracted residue near the fault site of cable 01-A-2. The insulation of cable 01-A-2 was found to contain several large particles between 15 and 17 mils in maximum dimension near the fault site. Similarly, the insulation of cable 03-A-2 also contained a number of large particles between 10 and 14 mils in maximum dimension.

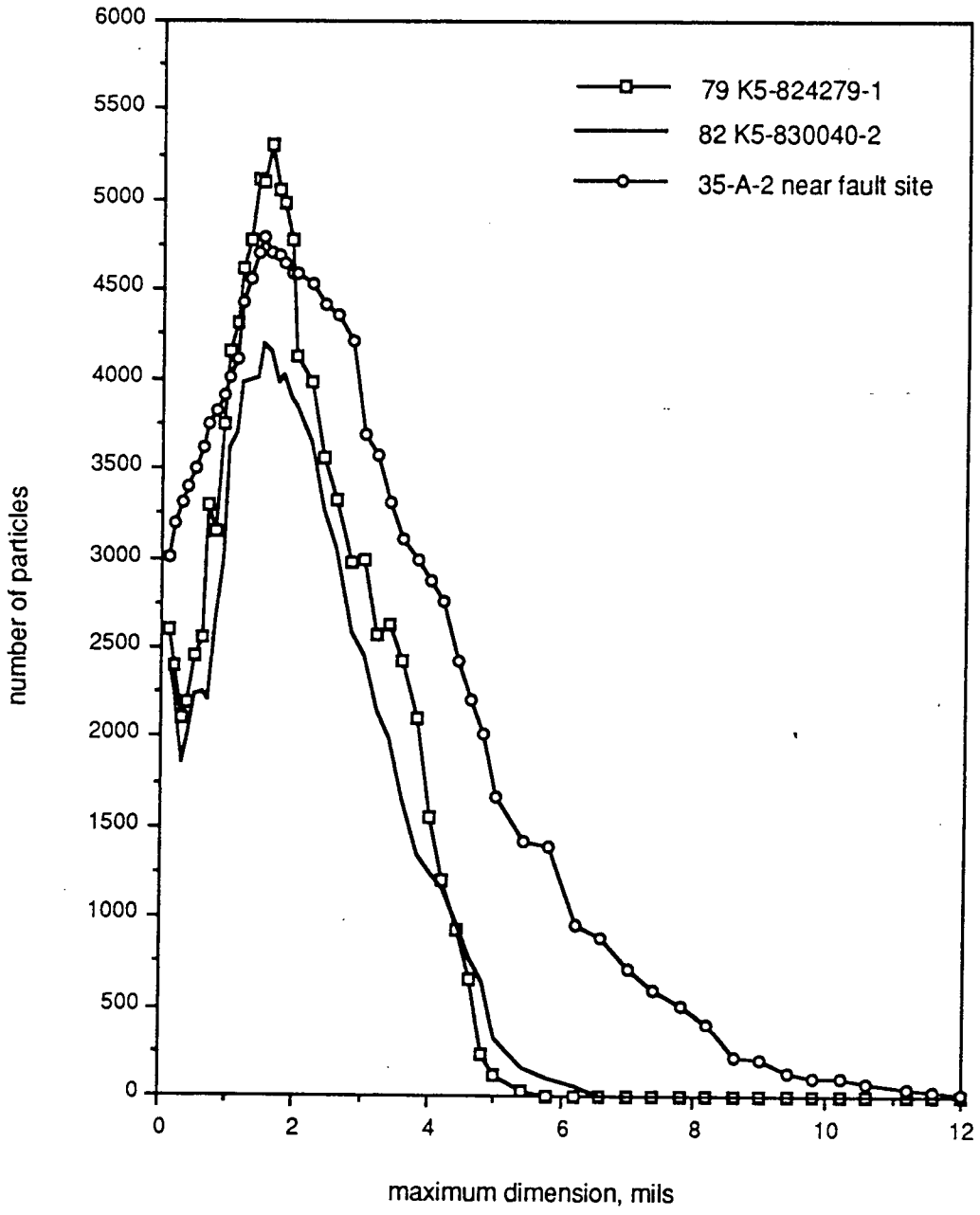

Figure 56. Size Distributions of Plasma-Extracted Inorganic Components of the Insulations, Comparing LOCA Tested Cable 35-A-2 to Non-Failed Vintages

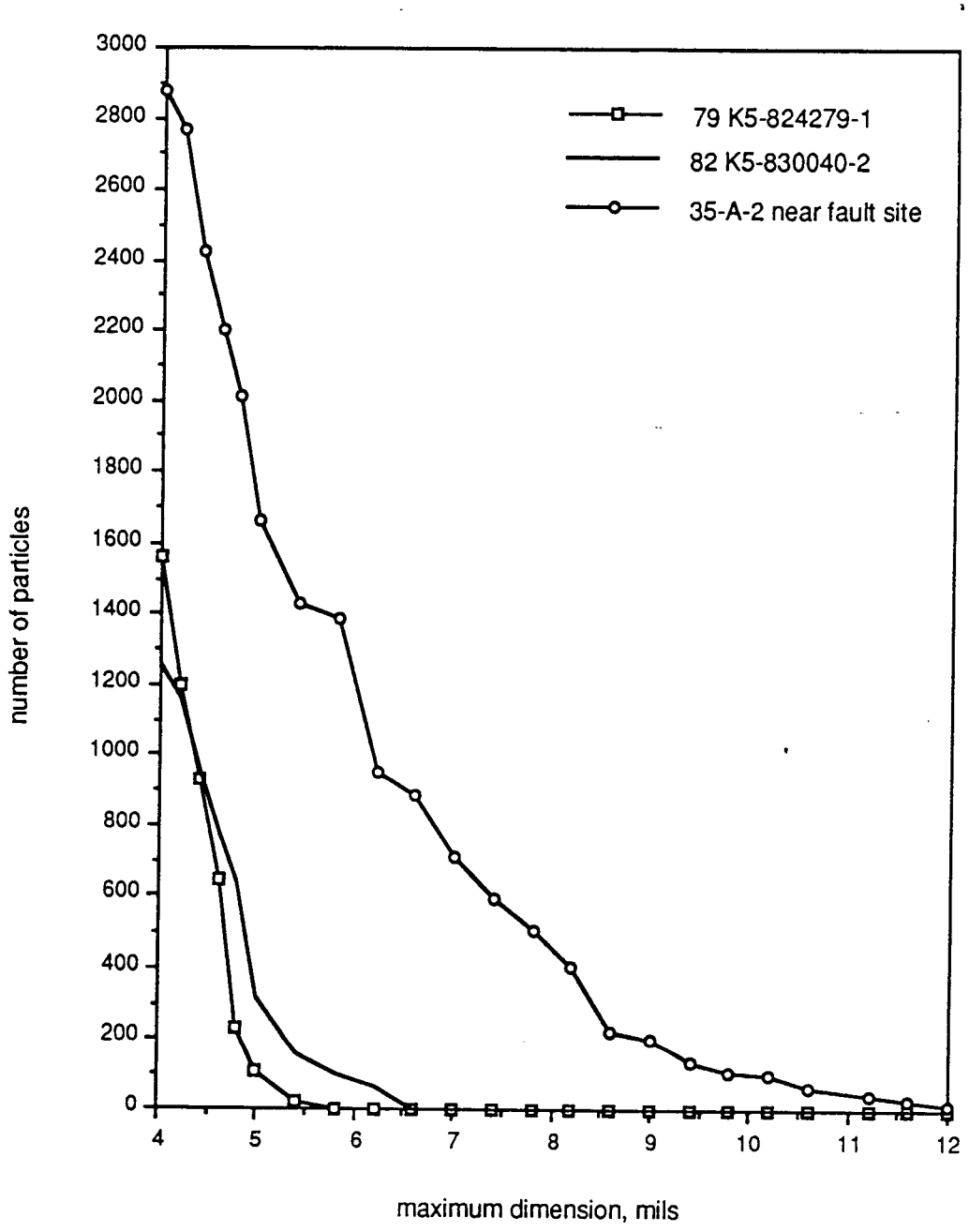

Figure 57. Size Distributions of Plasma-Extracted Inorganic Components of the Insulations, Comparing LOCA Tested Cable 35-A-2 to Non-Failed Vintages (Expanded Scale)

Figure 58. Plasma-Extracted Particles from the Insulation of Cable 35-A-2, Near the Fault Site, 100x Magnification

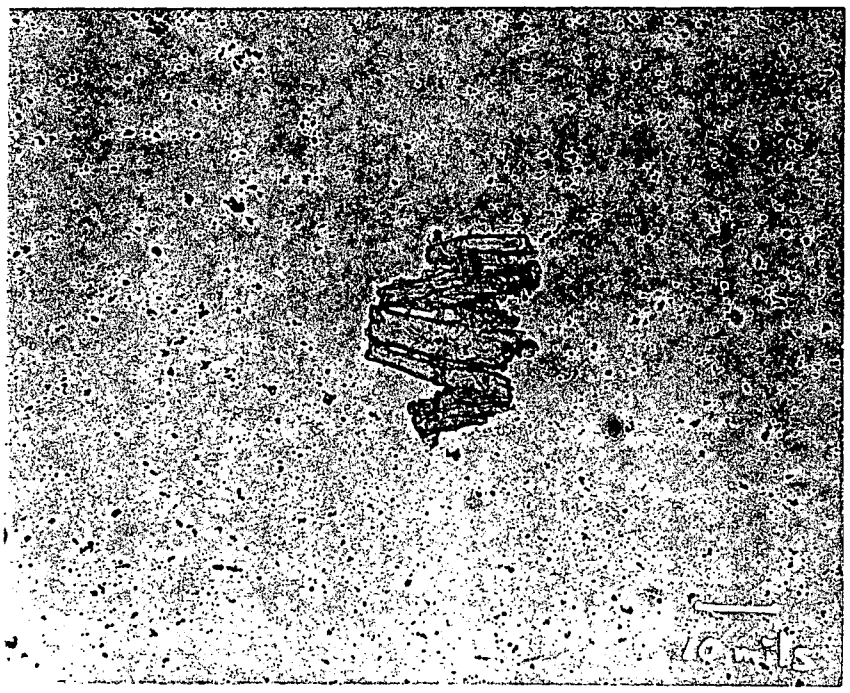

Figure 59. Plasma-Extracted Particles from the Insulation of Cable 35-A-2, Near the Fault Site, 100x Magnification

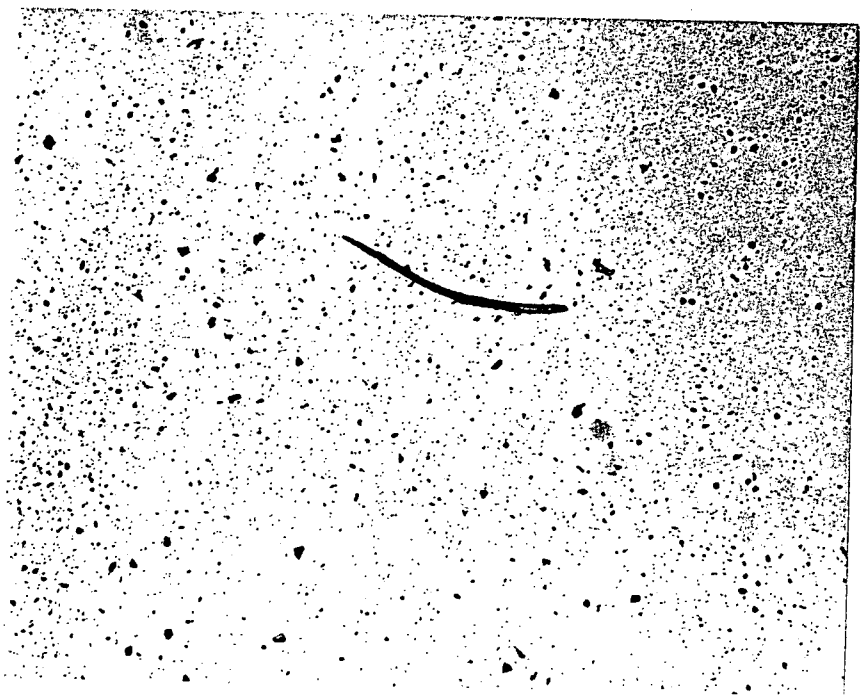

Figure 60. Plasma-Extracted Particles from the Insulation of Cable 01-A-2, Near the Fault Site, 100x Magnification

Following plasma-etching of the insulations, the conductor strands of the LOCA tested cable fault sites were inspected at the fault sites. A stereomicroscope was used with a magnification range of 10x through 40x. No anomalies in the conductor strands were found at any of the four fault sites examined in this manner. The conductors were found to be smooth, continuous, and without any protrusions.

6.0 CONCLUSIONS - ALL CONTRACTS

A series of installed cables supplied under contracts other than 80K6-825419 failed during in-situ electrical testing. Inspection of the majority of these cables, as listed in Table 14, indicated that the test failures occurred at sites where identifiable mechanical damage of the insulation had occurred. Pull-by damage could not be implicated as the causative factor for any of the failures that resulted from hipot testing. In all cases, the damage was sufficient that the dielectric integrity of the insulations had been compromised.

Other installed cables that failed during in-situ electrical testing failed for reasons other than identifiable mechanical damage or construction defects. These cables are identified in Table 15.

TABLE 14
CABLES THAT FAILED DUE TO INFLICTED MECHANICAL DAMAGE

2PS207B	1PM8J	2PM3806B	2PM3765B
	1PM2440B	1PM1835K	

TABLE 15
CABLES THAT FAILED DUE TO ANOMALOUS LARGE INORGANIC INSULATION COMPONENTS

1PM2445B	1PM2485B	2V1011B	1PM2080B
2RP1945-IB			

TABLE 16
CABLES THAT FAILED IN-SITU TESTING FOR WHICH NO FAULT SITE COULD BE LOCATED

1PM1661J	2PM3926B	2PV142B

Pyrolitic extraction of the insulations from the fault sites of the cables shown in Table 15 indicated that large particles of inorganic materials were present that were not otherwise present at remote locations in the same cables. These particles were identified with X-ray microanalysis and determined to be primarily antimony trioxide and silica. Antimony trioxide is a normal component of this insulation compound, as stated by the manufacturer, and serves as a component of the flame retardant system. Particles of antimony trioxide up to a maximum observed length of 59 mils were found at the fault site of one cable. Many had lengths in the range of 12 to 16 mils. Silica particles with a maximum dimension of 15 mils were also found near the fault sites of these cables. As shown in Figures 21, 22, 42, 43, 44, 45, 46, 54, 55, 58, 59, and 60, such antimony trioxide and silica particles are unique to the insulation compound corresponding to those cables that failed during in-situ electrical tests and supplied under contract 80K6-825419. This observation is further supported by the particle size measurements of the inorganic components of the various vintages of cable insulations as shown in Figures 47, 48, 51, 52, 56, and 57.

In all cases of electrical failures of the affected cables, large particles of inorganic material were associated with the insulation in the immediate vicinity of the fault sites. This is apparent from the previously discussed measurements and

observations as well as the comparison of inorganic components of the insulations from selected cables near and away from the fault sites as shown in Figures 49, 50, 51, and 52. It is unfortunate that the loss of insulation at the fault sites led to a loss of evidence that might otherwise have directly revealed its cause. On the other hand, if areas of the insulation within 30 - 60 mils of the fault site exhibit properties that are distinctly different from those at randomly selected, non-faulted areas of the same cable, then it is reasonable to assume that this evidence is a fair indicator of the conditions that prevailed at the fault site.

In an insulation compound of this type, no chemical bonds are formed between the base polymer (polyethylene) and the inorganic components with which it is blended. In medium voltage cable insulation compounds, for example, the clay component is subjected to a chemical surface treatment to promote the formation of chemical bonds. Silane coupling agents are typically used for this application. The latter process assures, or at least improves the chances for achieving intimate contact and good physical dispersion of the inorganic materials within the insulation compound. Without a surface treatment, it would be difficult, if not highly improbable, that a void-free interface between polyethylene and the clay particles could be formed. Furthermore, mechanical flexing of the cable, such as reeling, re-reeling, and pulling could further increase the size of interfacial gaps. Under elevated electrical stress conditions, the dielectric strength of the air in these gaps could be exceeded, thus leading to a localized dielectric breakdown of the cable insulation. In the experience of EIRC, this problem has been observed in clay-filled polyethylene insulated medium voltage cables that incorporated non-surface treated clays.

In the present case, silane coupling agents cannot be used to form chemical bonds between the polyethylene and antimony trioxide. In the experience of EIRC, there are no presently available chemical treatments available to promote such bonding.

An important aspect of the preparation of an insulation compound that is well mixed and void free is that the size of the inorganic components be as fine as reasonably possible, as supplied. While shear stresses encountered during mixing of an insulation compound may be quite high, this process cannot be relied upon to reduce the size of inorganic particles.

The source of silica in the insulations of the failed cables was not determined. Suggestions by the manufacturer that this may have arisen from thermal decomposition of the silicone rubber assembly tape, the glass fibers within this tape, or a silicone processing aid were shown to be inconsistent with the observed phenomena and conditions. While the cables contain inorganic colorants for identification purposes, it is unlikely that silica is an ingredient of one or more of these colorant systems. Silica, though it appears to be very white, has high transparency to visible light and is therefore inefficient as a colorant. Titanium dioxide is considerably more efficient, for example, as a white pigmenting agent. Silica may have been introduced as an adventitious impurity of the antimony trioxide. The latter is natural material that is refined from a mineral source. The majority of mineral species contain silica as a component or as an impurity. Since silica has excellent dielectric properties, its presence would not adversely alter the performance of an insulation compound, unless present in large particle size, as

previously discussed. Silica is commonly used as a reinforcement for other polymers, such as epoxy, in dielectric applications.

Large particles of antimony trioxide, shaped like those found in the insulations of the cables that failed during electrical testing, could not be created using a variety of experimental conditions in the laboratory. These experiments were designed to simulate the high temperatures developed when the fault sites were created and during some of the high voltage testing procedures used at EIRC to locate the fault sites in selected cable specimens. At the melting temperature of antimony trioxide, particles of this material were shown to coalesce with rounded shapes. The particles of this material found at the fault sites were observed to have sharp corners and a high aspect ratio, in many cases

Crosslinking density measurements of the insulations indicated that some differences were present between the three cable vintages and between faulted and non-faulted areas of the same cables. Differences between the crosslinking densities near and away from the fault sites of a given cable can be explained in terms of the localized thermal histories near the fault sites. Heating can lead to the breakdown of chemical bonds which would cause a reduction in crosslinking density such as that observed for cables 2V1011B and 1PM2080B. Localized heating can also lead to evaporation of the insulation. The non-crosslinked portion of the insulation would react more quickly, leaving a greater concentration of crosslinked material behind. This is consistent with the behavior shown in cables 1PM2485B and 1PM2445B. Differences between the crosslinking densities of the cables supplied under contracts 79K5-824279-1 and 82K5-830040-2 can be

explained in terms of the normal range of crosslinking density distributions along a given cable and from batch-to-batch of insulation compounds. Crosslinking is a statistical process that is affected by the exposure time to the radiation source, the molecular weight and molecular weight distribution of the polyethylene component of the insulation compound, and by other factors. Since each may vary in a given process/batch, there is typically a range of associated crosslinking density for a given product. In the experience of EIRC, variations of 10-15% are not uncommon.

Thermogravimetric analysis indicated that the insulation formulations were essentially identical from cable-to-cable for the 1980 cables that failed during in-situ electrical testing. In addition, these measurements indicated that the latter cable insulations were identical to those provided under contracts 79K5-824279-1 and 82K5-830040-2. These measurements further indicated that the insulation formulations were identical near and away from the fault sites of the affected cables.

Infrared spectroscopy indicated that the insulation compound contained no detectable organic additives that could be used to determine if the insulation compound had been altered during the 1979-1982 period. The only extractable material that could be identified with this technique was polyethylene, the insulation base polymer.

In summary, tests of the insulation compound indicated that the insulation formulation was uniform from the 1979-1982 time period. The failed cables appear to have suffered from localized deposits of anomalously large particles of, primarily, antimony

trioxide. In addition, silica particles were also uniquely associated with the fault sites of some of the cables that failed during in-situ testing. These particles were present with a size that is inconsistent with the manufacturer's claim that their extruder screen pack design prohibits the inclusion of particles larger than 4 mils into the insulation.

It should be noted that though the cables supplied under contract 80K6-825419 contained the anomalies addressed in this report, they were shown to pass the LOCA test regimen at TVA. Subsequent hi-pot testing of these cables showed that they, too, could be caused to fail due to the same anomaly. In the experience and opinion of EIRC, if TVA intends to continue its practice of in-situ hipot testing of low voltage cables at these stress levels then it should consider imposing more stringent requirements on its suppliers for cleanliness and dispersion of the insulation compounds used for these cables.